

# Cyclic Adenosine Monophosphate-Response Element-Binding Protein Mediates the Proangiogenic or Proinflammatory Activity of Gremlin

Michela Corsini, Emanuela Moroni, Cosetta Ravelli, Germán Andrés, Elisabetta Grillo, Imran H. Ali, Derek P. Brazil, Marco Presta, Stefania Mitola

**Objective**—Angiogenesis and inflammation are closely related processes. Gremlin is a novel noncanonical vascular endothelial growth factor receptor-2 (VEGFR2) ligand that induces a proangiogenic response in endothelial cells (ECs). Here, we investigated the role of the cyclic adenosine monophosphate-response element (CRE)-binding protein (CREB) in mediating the proinflammatory and proangiogenic responses of ECs to gremlin.

**Approach and Results**—Gremlin induces a proinflammatory response in ECs, leading to reactive oxygen species and cyclic adenosine monophosphate production and the upregulation of proinflammatory molecules involved in leukocyte extravasation, including chemokine (C-C motif) ligand-2 (Ccl2) and Ccl7, chemokine (C-X-C motif) ligand-1 (Cxcl1), vascular cell adhesion molecule-1 (VCAM-1), and intercellular adhesion molecule-1 (ICAM-1). Accordingly, gremlin induces the VEGFR2-dependent phosphorylation, nuclear translocation, and transactivating activity of CREB in ECs. CREB activation mediates the early phases of the angiogenic response to gremlin, including stimulation of EC motility and permeability, and leads to monocyte/macrophage adhesion to ECs and their extravasation. All these effects are inhibited by EC transfection with a dominant-negative CREB mutant or with a CREB-binding protein-CREB interaction inhibitor that competes for CREB/CRE binding. Also, both recombinant gremlin and gremlin-expressing tumor cells induce proinflammatory/proangiogenic responses in vivo that are suppressed by the anti-inflammatory drug hydrocortisone. Similar effects were induced by the canonical VEGFR2 ligand VEGF-A<sub>165</sub>.

**Conclusions**—Together, the results underline the tight cross-talk between angiogenesis and inflammation and demonstrate a crucial role of CREB activation in the modulation of the VEGFR2-mediated proinflammatory/proangiogenic response of ECs to gremlin. (*Arterioscler Thromb Vasc Biol.* 2014;34:136-145.)

**Key Words:** cyclic AMP response element-binding protein

Angiogenesis and inflammation are closely integrated processes.<sup>1-3</sup> Inflammatory cells may produce angiogenic cytokines, growth factors, and proteases that contribute to the formation of new vascular structures at the site of inflammation, tissue damage, or tumor growth.<sup>3,4</sup> Moreover, several proinflammatory cytokines may induce blood vessel formation via direct engagement of target endothelial cells (ECs) or indirectly by inducing leukocytes and ECs to produce proangiogenic mediators.<sup>5-7</sup> However, angiogenic factors, such as vascular endothelial growth factor (VEGF), angiopoietin-1 (Ang-1), and fibroblast growth factor-2 (FGF2), may elicit proinflammatory responses in ECs by upregulating the expression of cell adhesion molecules and inflammatory mediators involved in leukocyte recruitment and activation.<sup>8-10</sup> Thus, neovascularization and inflammation share several common signaling pathways and molecular mediators.

The cyclic adenosine monophosphate (cAMP)-response element-binding protein (CREB) is a bZip transcription factor

that forms homodimers or heterodimers with other CREB or activating transcription factor (ATF) family members and binds to specific cAMP-response element (CRE) promoter sites to regulate the transcription of numerous genes.<sup>11</sup> Several lines of evidence implicate CREB activation in angiogenesis and inflammation. CREB regulates the expression of several genes induced by hypoxia, such as VEGF<sup>12,13</sup> and its receptor.<sup>14,15</sup> Also, overexpression of a constitutively active form of CREB enhances tumor angiogenesis.<sup>16</sup> Conversely, VEGF induces CREB phosphorylation in ECs, thus increasing its transcriptional activity.<sup>16,17</sup> This capacity is shared by other angiogenic growth factors, including FGF2 and hepatocyte growth factor.<sup>18,19</sup> However, cyclooxygenase-2 upregulation induced by inflammatory cytokines in ECs as well as various pattern recognition receptor responses are mediated by CREB activation.<sup>20,21</sup>

Gremlin belongs to the cystine-knot protein family<sup>22,23</sup> and is expressed in several pathological conditions, including fibrotic

Received on: June 3, 2013; final version accepted on: October 28, 2013.

From the Department of Molecular and Translational Medicine, University of Brescia, Brescia, Italy (M.C., E.M., C.R., E.G., M.P., S.M.); Electron Microscopy Unit, Centro de Biología Molecular Severo Ochoa, Campus Cantoblanco, Madrid, Spain (G.A.); and Centre for Experimental Medicine, Queen's University Belfast, ICS-A, Grosvenor Road, Belfast BT12 6BA, UK (I.H.A., D.P.B.).

The online-only Data Supplement is available with this article at <http://atvb.ahajournals.org/lookup/suppl/doi:10.1161/ATVBAHA.113.302517/-/DC1>.

Correspondence to Stefania Mitola or Marco Presta, Department of Molecular and Translational Medicine, University of Brescia, Viale Europa 11, 25123 Brescia, Italy. E-mail [mitola@med.unibs.it](mailto:mitola@med.unibs.it) or [presta@med.unibs.it](mailto:presta@med.unibs.it)

© 2013 American Heart Association, Inc.

*Arterioscler Thromb Vasc Biol* is available at <http://atvb.ahajournals.org>

DOI: 10.1161/ATVBAHA.113.302517

Nonstandard Abbreviations and Acronyms	
<b>BMP</b>	bone morphogenic protein
<b>CAM</b>	chorionallantoide membrane
<b>cAMP</b>	cyclic adenosine monophosphate
<b>CREB</b>	cAMP-response element binding
<b>ECs</b>	endothelial cells
<b>HUVECs</b>	human umbilical vein endothelial cells
<b>ICAM-1</b>	intercellular adhesion molecule-1
<b>VCAM-1</b>	vascular cell adhesion molecule-1
<b>VEGF-A</b>	vascular endothelial growth factor-A
<b>VEGFR2</b>	vascular endothelial growth factor receptor 2

diseases<sup>24</sup> and cancer.<sup>25–27</sup> Gremlin acts as a bone morphogenic protein (BMP) antagonist by binding BMP2, BMP4, and BMP7.<sup>28</sup> Also, gremlin stimulates EC intracellular signaling and motility in a BMP-independent manner, leading to a potent angiogenic response *in vivo*.<sup>27,29</sup> This is because of the capacity of gremlin to bind and activate VEGF receptor-2 (VEGFR2), the main transducer of VEGF-mediated angiogenic signals.<sup>30,31</sup> Also, gremlin interacts with heparan-sulfate proteoglycans that act as functional gremlin coreceptors in ECs, affecting its productive interaction with VEGFR2.<sup>32</sup> However, at variance with heparin-binding VEGFs, gremlin does not interact with the coreceptor neuropilin-1.<sup>32</sup> Thus, gremlin is a novel proangiogenic VEGFR2 agonist distinct from canonical VEGFs.

Here, we demonstrate that gremlin induces a proinflammatory response in ECs by inducing the expression of various chemokines and cell adhesion molecules, causing a VEGFR2-mediated activation of CREB. In turn, CREB activation mediates the early phases of the angiogenic response to gremlin, including stimulation of EC motility and permeability, and leads to leukocyte-adhesion to ECs and their extravasation. In keeping with these observations, gremlin and gremlin-expressing tumor cells induce a proinflammatory or proangiogenic response *in vivo* that is suppressed by the anti-inflammatory drug hydrocortisone. These data point to a nonredundant role of CREB in mediating the EC response to gremlin and underline the tight cross-talk between angiogenesis and inflammation.

## Materials and Methods

Materials and Methods are available in the online-only Supplement.

## Results

### Gremlin Induces a Proinflammatory Response in ECs

Gremlin induces a potent angiogenic response *in vitro* and *in vivo*.<sup>27,30,33</sup> To get further insights on the proangiogenic activity of gremlin, we assessed the transcriptional profile of murine microvascular ECs (SIECs) stimulated by recombinant gremlin using Affymetrix MG-U74Av2 genechips (consisting of 22 690 probe sets, corresponding to  $\approx 15\,000$  genes). A preliminary analysis of the data indicates that a noticeable group of gremlin-induced genes was related to the inflammatory response, including various cytokines, chemokines, and leukocyte-adhesion molecules (Andres, article in preparation).

To confirm these observations, serum-starved SIECs were stimulated with recombinant gremlin and investigated by quantitative real time polymerase chain reaction analysis for the expression of the monocyte/macrophage chemotactic chemokine (C-C motif) ligand-2 (Ccl2) and Ccl7, the neutrophil chemoattractant chemokine (C-X-C motif) ligand-1 (Cxc11) and of the cell adhesion molecules vascular cell adhesion molecule-1 (VCAM-1) and intercellular adhesion molecule-1 (ICAM-1). Time-course analysis demonstrates the capacity of gremlin to induce an early upregulation of all the genes investigated, thus confirming its ability to induce a proinflammatory response in ECs. Similar results were obtained when SIECs were stimulated with the proangiogenic canonical VEGFR2 ligand VEGF-A<sub>165</sub> (Figure I in the online-only Data Supplement). In keeping with their capacity to trigger a proinflammatory response in ECs, gremlin and VEGF-A<sub>165</sub> stimulated also the production of cAMP and of reactive oxygen species (Figure II in the online-only Data Supplement).

### Gremlin Induces CREB Activation in ECs

CREB activation has been implicated in the regulation of growth factor-mediated inflammatory and vascular remodeling responses.<sup>16</sup> In SIECs, gremlin induces a dose-dependent phosphorylation of CREB (on Ser-133) and its rapid nuclear translocation (Figure 1A and 1B). This was paralleled by phosphorylation (on Ser-66) and nuclear translocation of the cross-reacting family member ATF-1<sup>34</sup> and was preceded by the phosphorylation and nuclear translocation of extracellular signal-regulated protein kinases 1 and 2 (ERK<sub>1/2</sub>; Figure 1B). Similar results were obtained by immunofluorescence analysis of SIECs that showed a perinuclear pCREB immunoreactivity on 10 minutes of stimulation with gremlin and a nuclear staining after 20 minutes (Figure 1D). In keeping with previous observations,<sup>16,17</sup> CREB phosphorylation and nuclear translocation were observed also after SIEC stimulation by VEGF-A<sub>165</sub> (Figure 1B and 1D). This occurred with more rapid kinetics when compared with gremlin stimulation, possibly as a consequence of the different in-plane intermolecular attractive interactions after VEGFR2 recognition by the 2 ligands.<sup>31</sup>

The capacity of gremlin to induce CREB activation was further assessed in starved human umbilical vein endothelial cells (HUVECs) exposed to gremlin for 0 to 60 minutes by electrophoretic mobility shift assay using a biotin-labeled CRE oligonucleotide probe. As anticipated, gremlin induces the formation of the CREB/CRE complex in a time-dependent manner (Figure 1C). Complex formation was significantly inhibited by a 100-fold excess of the unlabeled CRE probe, but not of an unlabeled mutated probe; also, incubation with an anti-CREB antibody caused the supershift of the complex (Figure 1C). Finally, we established an *in situ* CREB/DNA-binding assay to visualize the CRE-binding activity of CREB directly in cells or tissue sections (see Materials and Methods section in the online-only Data Supplement). To this purpose, gremlin-treated HUVECs were fixed, permeabilized, and incubated for 1 hour with a Cy5-labeled oligoprobe containing the palindromic or the mutated CRE sequence. As shown in Figure 1E, the Cy5-labeled palindromic CRE oligoprobe binds the nuclear CREB of gremlin-stimulated cells, whereas the mutated oligoprobe

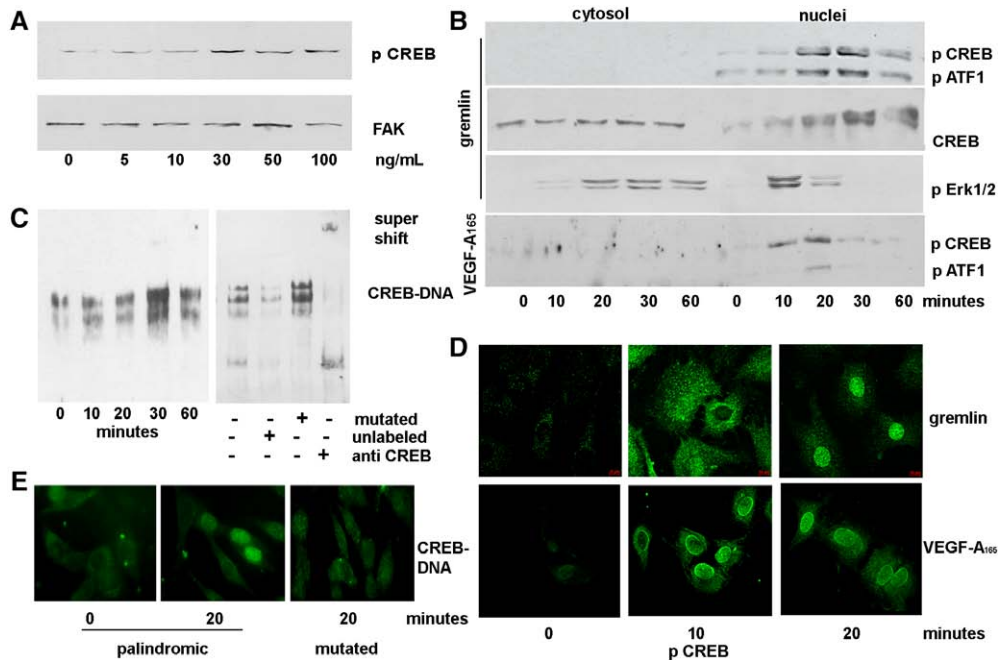


**Figure 1.** Gremlin induces cAMP-response element (CRE)-binding protein (CREB) activation. **A**, Cell lysates were prepared from murine microvascular ECs (SIECs) stimulated for 15 minutes with 0, 5, 10, 30, 50, and 100 ng/mL of recombinant gremlin. Twenty micrograms of aliquots were probed by Western blotting with anti-pCREB antibodies. Uniform loading of the gels was confirmed by incubation of the membranes with anti-FAK antibodies. **B**, SIECs were stimulated for 0 to 60 minutes with 50 ng/mL of gremlin or with 50 ng/mL of vascular endothelial growth factor-A (VEGF-A<sub>165</sub>). Then, nuclear (5.0 µg) and cytoplasmic (10 µg) extracts were probed by Western blotting with anti-pCREB, anti-CREB, and anti-ERK<sub>1/2</sub> antibodies. **C**, SIECs were treated for 0 to 60 minutes with 50 ng/mL of gremlin. Then, nuclear extracts (2.0 µg) were incubated with a biotin-labeled CREB double-stranded DNA oligonucleotide probe (**left**). Also, 2.0 µg of nuclear extracts of SIECs treated for 20 minutes with 50 ng/mL of gremlin were incubated with a biotin-labeled CREB double-stranded DNA oligonucleotide probe in the absence or in the presence of a molar excess of the unlabelled CREB probe or of a mutant CREB probe or in the presence of anti-CREB antibodies (**right**). The protein-DNA complexes were analyzed by electrophoretic mobility shift assay onto a native 6% polyacrylamide gel. **D**, Serum-starved SIECs were incubated for 0 to 20 minutes with 50 ng/mL of gremlin or VEGF-A<sub>165</sub> and immunostained with anti-pCREB antibody followed by anti-rabbit Alexa488. Samples were analyzed using a Zeiss Axiovert 200M epifluorescence microscope equipped with Apotome system and a Plan-Apochromat 63x/1.4 NA oil objective. Data in **B** and **D** indicate that gremlin induces a slower CREB nuclear translocation compared with VEGF-A<sub>165</sub>. **E**, Serum-starved human umbilical vein endothelial cells were incubated for 0 or 20 minutes with 50 ng/mL of gremlin. Then, cells were fixed and stained with a Cy5-labeled oligoprobe containing the palindromic CRE sequence or a mutated sequence. The Cy5-labeled palindromic CRE oligoprobe binds the nuclear DNA of gremlin-stimulated cells, whereas the mutated oligoprobe was ineffective. Analysis was performed using a Zeiss Axiovert 200M epifluorescence microscope equipped with a Plan-Apochromat 63x/1.4 NA oil objective. Results are representative of 3 independent experiments.

was ineffective. Together, these results confirm the specificity of CREB/CRE binding after gremlin stimulation in ECs.

### VEGFR2 Mediates CREB Activation by Gremlin in ECs

Gremlin is a noncanonical ligand of the major proangiogenic receptor VEGFR2 without exerting any interaction with VEGFR1.<sup>30</sup> To assess whether the capacity of gremlin to induce CREB activation is attributable to a VEGFR2-mediated effect, SIECs were pretreated with the tyrosine kinase VEGFR2 inhibitor SU5416<sup>30</sup> and incubated for 15 minutes with gremlin. As shown in Figure 2A, SU5416 fully prevents CREB activation as assessed by ELISA, thus confirming that CREB activation is part of the VEGFR2-mediated proangiogenic response elicited by gremlin in ECs. Relevant to this point, gremlin induces CREB phosphorylation also in VEGFR2-expressing smooth muscle cells with no effect on VEGFR1-expressing peripheral blood mononuclear cells (Figure III in the online-only Data Supplement).

As described above, ERK<sub>1/2</sub> phosphorylation precedes CREB activation in gremlin-treated ECs (see Figure 1B). A 60-minute preincubation with the MAP kinase kinase inhibitor PD98059,<sup>12</sup> the p38 mitogen activated protein kinase

inhibitor SB202190,<sup>12</sup> or the Src inhibitor PP2<sup>12</sup> all prevent CREB phosphorylation and DNA binding triggered by gremlin (Figure 2A and 2B).

Together, these data indicate that activation of the mitogen activated protein kinase pathway after VEGFR2 engagement plays a pivotal role in CREB activation by gremlin in ECs.

### CREB Mediates the Early Phases of the Angiogenic Response of ECs to Gremlin

Increased permeability and acquisition of a promigratory phenotype are among the earliest events that occur in ECs after stimulation by proangiogenic factors, including VEGF. Accordingly, previous observations had shown that gremlin elicits a motogenic response in ECs both when administered as a recombinant protein or when produced by gremlin-over-expressing tumor cells.<sup>33</sup> However, no data were available about a possible effect of gremlin on EC permeability.

Here, confluent HUVEC monolayers plated on Transwell membrane support were treated for 24 hours with the conditioned medium from human breast carcinoma MCF7 cells stably transfected with the human gremlin cDNA (gremlin-MCF7 cells) or with the empty vector (mock-MCF7 cells).<sup>33</sup> Then,



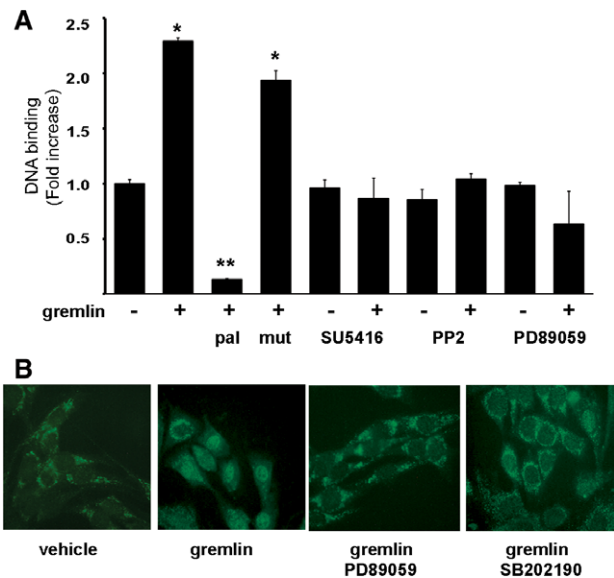


**Figure 2.** Vascular endothelial growth factor receptor-2 (VEGFR2) mediates cAMP-response element-binding protein (CREB) activation by gremlin. **A**, Murine microvascular endothelial cells were pretreated for 1 hour with the tyrosine kinase VEGFR2 inhibitor SU5416 (5.0  $\mu\text{mol/L}$ ), the MAP kinase kinase inhibitor PD89059 (25  $\mu\text{mol/L}$ ), the p38 mitogen activated protein kinase inhibitor SB202190 (25  $\mu\text{mol/L}$ ), or the Src inhibitor PP2 (5.0  $\mu\text{mol/L}$ ) and incubated for further 15 minutes in the absence or in the presence of 50 ng/mL of gremlin. Then, 5  $\mu\text{g}$  of nuclear extract was probed for CREB-binding activity with the pCREB Transcription Factor ELISA kit. Extracts from gremlin-treated cells were probed also in the presence of a molar excess of the unlabeled CREB probe (pal) or of a mutant CREB probe (mut; mean values  $\pm$  SD;  $n=3$ ; \* $P<0.05$ ; \*\* $P<0.01$ ; Student  $t$  test). **B**, Cells were immunostained with an anti-pCREB antibody followed by anti-rabbit Alexa488. Analysis was performed using a Zeiss Axiovert 200M epifluorescence microscope equipped with a Plan-Apochromat 63x/1.4 NA oil objective.

50  $\mu\text{g}$  of biotin-labeled bovine serum albumin were added to the upper Transwell chamber, and the amount of bovine serum albumin diffused to the lower chamber through the HUVEC monolayer was quantified after 90 minutes. Gremlin significantly affects HUVEC permeability, as demonstrated by the 2-fold increase of biotin-labeled bovine serum albumin detectable in the lower wells treated with the conditioned medium from gremlin-MCF7 cells when compared with mock cells (Figure 3A). The loss of EC barrier integrity was confirmed by immunofluorescence analysis of gremlin-treated HUVEC monolayers using antibodies against the major endothelial adherens junction protein vascular endothelial-cadherin and the tight junction-associated protein zonula occludens ZO-1. When compared with control cells, cells treated with gremlin were characterized by an increased number of intercellular gaps and by the delocalization of vascular endothelial-cadherin and ZO-1 from the cell junctions to the cytoplasm (Figure 3B). Similar to that described for VEGF- $A_{165}$ ,<sup>35</sup> the nitric oxide synthase inhibitor NG-nitro-L-arginine methyl ester (L-NAME) prevented EC junction disruption in gremlin-stimulated cells (Figure IV in the online-only Data Supplement). In agreement with these observations, both recombinant gremlin and VEGF- $A_{165}$  similarly affected blood vessel permeability in vivo when tested subcutaneously (s.c.) in the Miles assay<sup>36</sup> (Figure 3C and C').

Inhibition of CREB activation after transient transfection with the dominant-negative bZIP domain mutant ACREB<sup>37</sup> (Figure 3A') prevents the increase of permeability induced by gremlin in HUVECs (Figure 3A). Similarly, ACREB overexpression significantly inhibited the chemokinetic response elicited by gremlin or VEGF- $A_{165}$  in HUVECs as assessed by time-lapse video microscopy (Figure 3D) and the chemotactic activity exerted by gremlin on SIECs in a Boyden chamber assay (Figure VA in the online-only Data Supplement). Accordingly, a CRE-decoy 24-mer oligonucleotide<sup>38</sup> caused a dramatic reduction of the chemotactic response of HUVECs to gremlin (Figure VB in the online-only Data Supplement) with no effect on their adhesive capacity (data not shown).

These data point to a functional role of CREB in the early phases of the angiogenic response to gremlin by affecting EC permeability and motility.

### Gremlin Causes CREB-Dependent Leukocyte Extravasation

Leukocyte infiltration is a common feature of inflammation, angiogenesis, and cancer. It involves a sequence of VCAM-1 and ICAM-1-mediated adhesive events between leukocytes and endothelial receptors that culminates in leukocyte extravasation.<sup>39</sup> Previous observations had shown a direct or indirect role of CREB in mediating VCAM-1 and ICAM-1 upregulation in ECs.<sup>37,38,40</sup> To assess whether CREB activation is involved in the modulation of VCAM-1 and ICAM-1 expression by gremlin, mock- and ACREB-transfected HUVECs were treated with the conditioned medium from mock- or gremlin-MCF7 cells. After 24 hours, ICAM-1 and VCAM-1 transcript and protein levels were assessed by quantitative real time polymerase chain reaction and flow cytometry analysis, respectively. As shown in Figure 4A and 4B, ACREB overexpression hampered ICAM-1 and VCAM-1 upregulation triggered by gremlin with no effect on the expression of other EC genes, for example, platelet endothelial cell adhesion molecule-1. Similarly, ACREB overexpression prevented ICAM and VCAM-1 upregulation triggered by VEGF- $A_{165}$  in ECs (Figure VI in the online-only Data Supplement).

Given the role of ICAM-1 and VCAM-1 in mediating monocyte-EC adhesion and transmigration, we evaluated the adhesion of human monocytic THP-1 cells to gremlin-treated ECs. To this purpose, mock- and ACREB-transfected HUVECs were stimulated for 24 hours with the conditioned medium from mock-MCF7 or gremlin-MCF7 cells and incubated for 1 hour with LPS-activated THP-1 cells. The results demonstrate that gremlin significantly increases THP-1 cell adhesion to the EC monolayer ( $77 \pm 17$  versus  $135 \pm 15$  cells/field for control and gremlin-treated cells, respectively). As anticipated, this increase was prevented by coincubation with neutralizing monoclonal antibodies against ICAM-1 or VCAM-1, as well as by transient ACREB transduction in HUVECs (Figure 4C). Similar results were obtained when mock and ACREB-HUVECs were stimulated with recombinant gremlin or VEGF- $A_{165}$  (Figure VII in the online-only Data Supplement).

Next, we evaluated the effect of endothelial CREB activation by gremlin on leukocyte diapedesis. Mock- and ACREB-transfected HUVECs were plated on a Transwell membrane

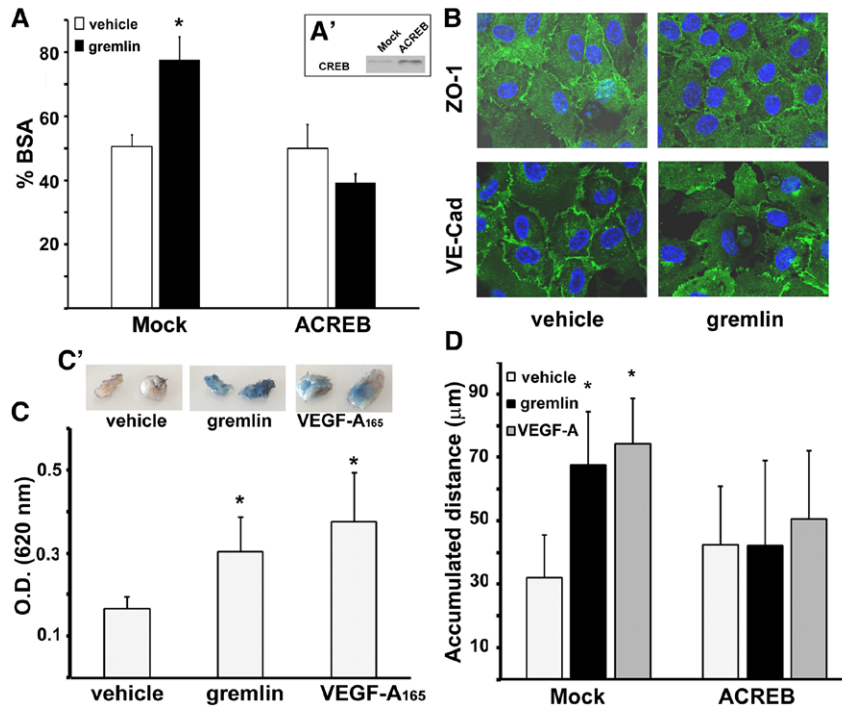


**Figure 3.** cAMP-response element-binding protein (CREB) modulates gremlin-induced endothelial cell (EC) permeability and motility. **A**, Mock- and ACREB-human umbilical vein endothelial cells (HUVECs) were plated at confluence on Transwell and treated with the conditioned medium from mock-MCF7 or gremlin-MCF7 cells for 24 hours. To measure EC permeability, biotin-bovine serum albumin (BSA) was added to the top chamber at 50  $\mu$ g/well. After 90 minutes, the top chamber was removed, and biotin-BSA was measured in the lower chamber with horseradish peroxidase-conjugated streptavidin. **A'**, Twenty-microgram aliquots of mock and ACREB-HUVEC lysates were probed by Western blotting with anti-CREB antibodies. **B**, Confluent HUVECs were incubated with vehicle or 50 ng/mL of gremlin, fixed with 3% paraformaldehyde, and permeabilized with 0.2% Triton X-100. Then, cells were incubated with anti-zonula occludens (ZO)-1 or anti-vascular endothelial-cadherin (VE-Cad) antibodies followed by anti-mouse Alexa 488 and nuclei were counterstained with 4',6-diamidino-2-phenylindole. Analysis was performed using a Zeiss Axiovert 200M epifluorescence microscope equipped with Apotome system and a Plan-Apochromat 63x/1.4 NA oil objective. Note that the cell-cell contact localization of ZO-1 and VE-Cad is lost in gremlin-treated cells. **C**, Systemic (i.v.) administration of Evans blue in C57BL/6 mice was followed by intradermal injection of vehicle or 50 ng of gremlin or vascular endothelial growth factor-A (VEGF-A<sub>165</sub>). Evans blue leakage was assessed after 20 minutes (representative images are shown in **C'**), and quantification of extravasated dye was assessed by formamide extraction. **D**, Mock and ACREB-HUVECs were seeded in M199 plus 5% fetal calf serum. Then, cells were stimulated with 50 ng/mL of gremlin or VEGF-A<sub>165</sub>, and cell motility was assessed by time-lapse videomicroscopy using an inverted photomicroscope (Zeiss Axiovert 200M) equipped with an LD A PLAN 20X/0.30PH1 objective. Constant temperature (37°C) and P<sub>CO</sub><sub>2</sub> (5%) were maintained throughout the experimental period by means of heatable stage and climate chamber. Phase-contrast snap photographs were digitally recorded for 240 minutes. Cell paths (15–20 cells per experimental point) were generated from centroid positions, and migration parameters were analyzed with the Chemotaxis and Migration Tool of ImageJ Software (<http://rsbweb.nih.gov/ij/>). Accumulated distances (in  $\mu$ m) are shown in **D**. \* $P$ <0.05; Student *t* test.

support and cocultured with mock-MCF7 or gremlin-MCF7 cells seeded in the lower chamber. After 24 hours, LPS-activated THP-1 cells were added to the upper chamber in the absence or in the presence of neutralizing anti-ICAM-1 or anti-VCAM-1 antibodies and allowed to transmigrate for the next 16 hours. The amount of THP-1 cells transmigrated throughout the HUVEC monolayer was 6-fold higher in the presence of gremlin-MCF7 cells in the lower chamber than in the presence of mock-MCF7 cells. Also, THP-1 cell transmigration was prevented by neutralizing anti-ICAM-1 or anti-VCAM-1 antibodies. Moreover, inhibition of CREB activation in HUVECs by ACREB transduction significantly reduced THP-1 adhesion and transmigration (Figure 4D). It must be pointed out that, in the absence of the HUVEC monolayer, THP-1 cells showed a similar, limited migratory response toward mock-MCF7 and gremlin-MCF7 cells (data not shown). This observation suggests that THP-1 cell transmigration is driven by a gremlin-induced chemotactic stimulus of EC origin rather than a direct chemotactic effect. Indeed, as described above, gremlin upregulates the expression of a

variety of chemokines in ECs that may be responsible for the observed THP-1 cell recruitment. In keeping with this hypothesis, gremlin-driven THP-1 cell transmigration through the HUVEC monolayer was significantly reduced by the pan-chemokine inhibitor M3, a murine  $\gamma$ -herpesvirus 68 protein antagonist for human and mouse CC, CXC, and CX3C chemokines<sup>41</sup> (Figure VIII in the online-only Data Supplement). Together the data indicate that gremlin stimulates monocyte transmigration by acting on ECs and inducing the coordinate upregulation of chemokine production and the CREB-dependent expression of the cell adhesion molecules VCAM-1 and ICAM-1 on the EC surface. This is paralleled by increased CREB-dependent EC permeability and acquisition of a motile phenotype.

On this basis, we evaluated the capacity of gremlin to induce a CREB-dependent leukocyte extravasation in vivo. In a first set of experiments, CREB activation by gremlin was assessed in the chick embryo chorionallantoide membrane (CAM) by the *in situ* CREB/DNA-binding assay described above. To this aim, CAMs were treated with gremlin (100 ng/implant) for 20 minutes. Then,

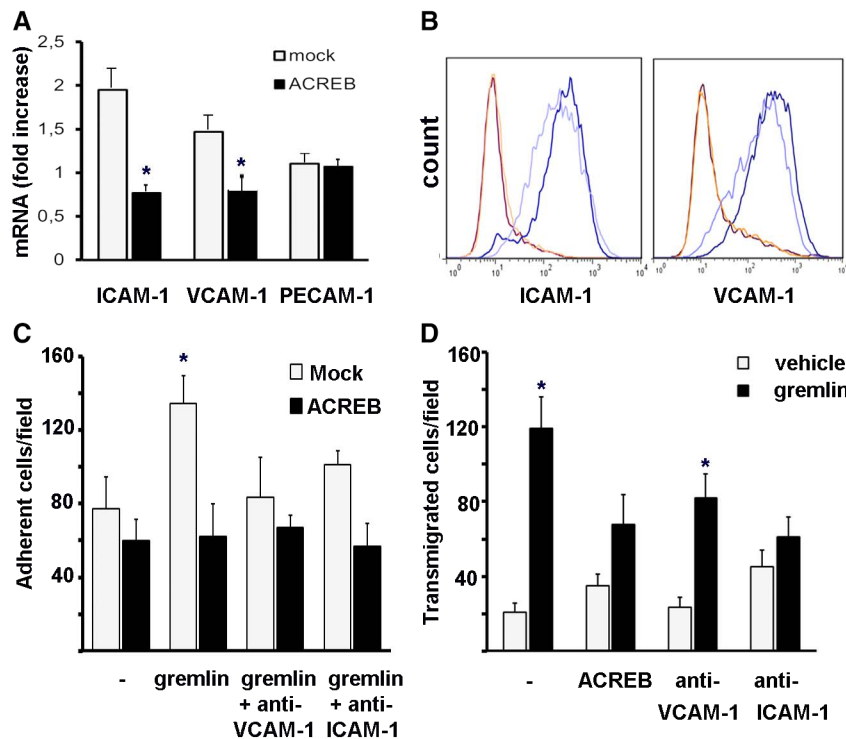


**Figure 4.** cAMP-response element-binding protein (CREB) mediates leukocyte extravasation induced by gremlin. **A** and **B**, Mock- and ACREB-transfected human umbilical vein endothelial cells (HUVECs) were treated for 24 hours with the conditioned medium from mock- or gremlin-MCF7 cells. Then, intercellular adhesion molecule-1 (ICAM-1), vascular cell adhesion molecule-1 (VCAM-1), and platelet endothelial cell adhesion molecule-1 mRNA levels were assessed by quantitative real-time polymerase chain reaction analysis (**A**), whereas ICAM-1 and VCAM-1 protein levels were quantified by flow cytometry analysis (orange line: mock-HUVECs stimulated by mock-MCF7; red line: ACREB-HUVECs stimulated by mock-MCF7; dark blue line: mock-HUVECs stimulated by gremlin-MCF7; blue line ACREB-HUVECs stimulated by gremlin-MCF7; **B**). **C**, Also, HUVECs treated as described above were incubated with lipopolysaccharides (LPS)-activated THP-1 cells for 1 hour. At the end of the incubation, THP-1 cells adherent to the endothelium were counted in 5 random fields using Zeiss Axiovert 200M epifluorescence microscope equipped with LD A PLAN 20X/0,30PH1 objective. When indicated, HUVECs were pretreated for 1 hour with neutralizing antibodies against ICAM-1 or VCAM-1 before incubation with monocyte THP-1 cells. Data are the mean $\pm$ SD of 3 determinations. **D**, Mock- and ACREB-transfected HUVECs were plated on a Transwell membrane support and cocultured for 24 hours with mock-MCF7 or gremlin-MCF7 cells seeded in the lower chamber. LPS-activated THP-1 cells were added to the upper chamber in the absence or in the presence of neutralizing anti-ICAM-1 or anti-VCAM-1 antibodies. Transmigrated THP-1 cells were counted in 5 random fields using Zeiss Axiovert 200M epifluorescence microscope equipped with LD A PLAN 20X/0,30PH1 objective. Data are the mean $\pm$ SD of 3 wells (\* $P$ <0.05; Student  $t$  test).

frozen tissue sections were incubated with the Cy5-labeled palindromic CRE oligoprobe and analyzed by immunofluorescence microscopy. As shown in Figure 5A, the Cy5-labeled palindromic CRE oligoprobe binds EC nuclei in gremlin-stimulated CAMs but not in control CAMs. The specificity of interaction was confirmed by the lack of nuclear staining when gremlin-treated CAMs were incubated with a Cy5-oligoprobe containing a mutation in the CRE sequence. These observations further confirm that CREB is a downstream molecule activated in vivo by gremlin in ECs. Next, alginate beads loaded with gremlin or VEGF-A<sub>165</sub> were implanted onto the CAMs at 11 days of development. As anticipated, both gremlin and VEGF-A<sub>165</sub> triggered the recruitment of a robust inflammatory cell infiltrate in the CAM stroma that was prevented by the topic administration of a CREB-binding protein-CREB interaction inhibitor that suppresses the transcriptional activity of CREB<sup>42</sup> (Figure 5B and 5C).

### Gremlin-Expressing Tumor Cells Induce a Proinflammatory/Proangiogenic Response In Vivo

To get further insights on the role of inflammation in gremlin-driven neovascularization, we compared the capacity of

gremlin and VEGF-A<sub>165</sub> to induce a proangiogenic response in the classical in vivo murine Matrigel plug angiogenesis assay<sup>43</sup> in the presence of the anti-inflammatory drug hydrocortisone. After 7 days, immunofluorescence and quantitative real time polymerase chain reaction analyses of the plugs<sup>43</sup> revealed a significant increase of the expression of the endothelial marker CD31 and of the pan-leukocyte marker CD45 both in gremlin and VEGF-A<sub>165</sub> plugs when compared with control plugs (Figure 6A). As anticipated, hydrocortisone prevented the recruitment of infiltrating cells and the neovascular response triggered by both VEGFR2 ligands (Figure 6B).

Gremlin is expressed by tumor and stromal cells in different human cancers.<sup>26</sup> On this basis, alginate beads loaded with the conditioned medium from mock-MCF7 or gremlin-MCF7 cells were implanted onto the CAMs. Similar to recombinant gremlin or VEGF-A<sub>165</sub>, the conditioned medium of gremlin-MCF7 cells induced a potent angiogenic response (Figure IXA in the online-only Data Supplement) that was paralleled by the recruitment of inflammatory cells in the stroma among the newly formed blood vessels (Figure IXB in the online-only Data Supplement). Again, hydrocortisone inhibited this coordinated



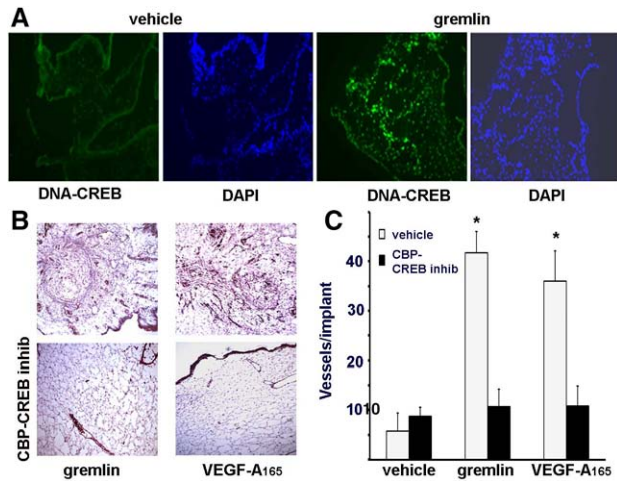


**Figure 5.** cAMP-response element-binding protein (CREB) mediates leukocyte recruitment and angiogenesis induced by gremlin in the chick embryo chorionallantoic membrane (CAM). **A**, CAMs at day 11 of development were treated with 100 ng/egg of gremlin or vehicle for 20 minutes and examined for CREB activation. To this purpose, frozen tissue sections were incubated with Cy5-labeled oligoprobe containing the palindromic CRE sequence and analyzed by immunofluorescence microscopy. Analysis was performed using a Zeiss Axiovert 200M epifluorescence microscope equipped with a ACROPLAN 10X/0.25 objective. Nuclei are highlighted by 4',6-diamidino-2-phenylindole (DAPI) counterstaining. **B**, Alginate pellets containing 100 ng of recombinant gremlin or vascular endothelial growth factor-A (VEGF-A)<sub>165</sub> were implanted on the top of chick embryo CAMs at day 11 of development in the absence or in the presence of 5.0  $\mu$ M of CREB-binding protein (CBP)-CREB interaction inhibitor. After 3 days, paraffin-embedded sections of the CAMs were stained with hematoxylin/eosin and analyzed using a Zeiss Axiovert 200M epifluorescence microscope equipped system and ACROPLAN 10X/0.25 (**top**) and LD A PLAN 20X/0.30PH1 (**bottom**) objectives. Note the presence of an abundant inflammatory cell infiltrate in the areas of gremlin and VEGF-A<sub>165</sub>-induced neovascularization (**top**) abolished by treatment with the CBP-CREB interaction inhibitor (**bottom**). **C**, Alginate pellets containing 100 ng of recombinant gremlin or VEGF-A<sub>165</sub> were assessed for their angiogenic capacity in the absence or in the presence of the CBP-CREB interaction inhibitor. Data (7–10 eggs per group) represent the number of vessels converging toward the alginate implant and are expressed as mean $\pm$ SD. \*statistically different from the vehicle group;  $P<0.05$ .

proinflammatory/neovascular response, further implicating inflammatory cells/mediators in gremlin-induced neovascularization (Figure IXA in the online-only Data Supplement).

Next, we assessed the effect of gremlin in a tumor angiogenesis assay. To this purpose, Matrigel embedded mock-MCF7 or gremlin-MCF7 cells were implanted s.c. in nu/nu male mice. Anti-nitro-tyrosine immunostaining of the implants performed at day 7 after injection demonstrates that gremlin-MCF7 cells induce NO production in tumor grafts (Figure 7A). Accordingly, gremlin-MCF7 xenografts were characterized by the presence of several CD31-positive blood vessels and of an abundant CD45-positive leukocyte infiltrate when compared with mock-MCF7 implants as shown by immunofluorescence and quantitative real time polymerase chain reaction analyses (Figure 7B and 7C). A further characterization of infiltrating cells showed that recruited leukocytes mainly consist of mature F4/80<sup>+</sup> macrophages and CD11b<sup>+</sup> monocytes with rare neutrophils (Figure 7B). Again, the

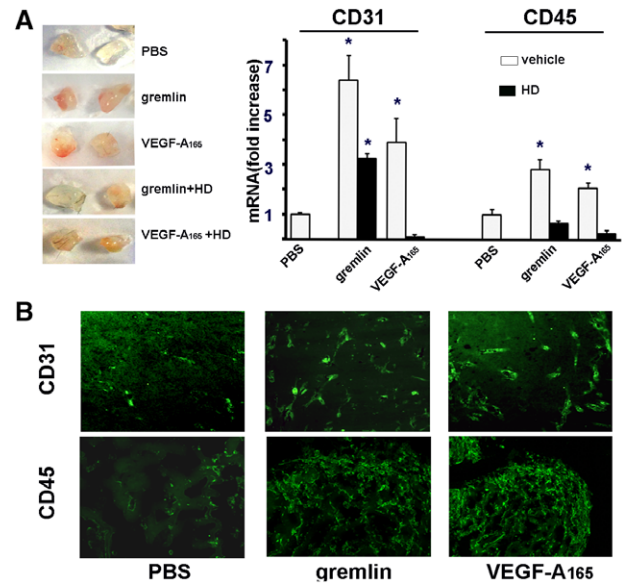


**Figure 6.** Gremlin exerts a potent proangiogenic activity in vivo. **A**, Matrigel plugs containing phosphate buffer saline or 1.0  $\mu$ g/mL of gremlin or vascular endothelial growth factor-A<sub>165</sub> were implanted s.c. in mice in the absence or in the presence of 10  $\mu$ g of hydrocortisone (HD). After 1 week, plugs were harvested, and quantification of CD31<sup>+</sup> endothelial cells and CD45<sup>+</sup> infiltrating leukocytes was performed by quantitative real time polymerase chain reaction analysis. Briefly, Matrigel plugs were weighed, homogenized in TRIzol solution, added with  $1 \times 10^4$  human cells per mg of plug and assessed for mCD31, mCD45, and hGAPDH expression levels by RT-qPCR. Data are the mean $\pm$ SEM of 7 plugs and are expressed as mCD31/hGAPDH and mCD45/hGAPDH mRNA ratios (\* $P<0.05$ ). **B**, Immunofluorescence analysis with anti-CD31 and anti-CD45 antibodies was performed on plug sections using a Zeiss Axiovert 200M epifluorescence microscope equipped with Apotome system and an LD A PLAN 20X/0.30PH1 objective.

administration of hydrocortisone prevented the inflammatory response and neovessel formation triggered by gremlin-MCF7 xenografts (Figure 7A–7C). Together, our findings support the notion that inflammatory responses are relevant for gremlin-dependent neovascularization.

## Discussion

Neovascularization and inflammation share common signaling pathways and molecular mediators. Several proinflammatory cytokines may induce blood vessel formation via a direct engagement of target ECs or indirectly by inducing leukocytes and ECs to produce proangiogenic mediators.<sup>44</sup> Conversely, angiogenic factors may elicit a proinflammatory signature in ECs,<sup>10,45</sup> causing the upregulation of cell adhesion molecules and inflammatory mediators that leads to the recruitment of proangiogenic leukocytes at the site of injury. Here, we show that the proangiogenic activity of gremlin is dependent on its direct effect on EC behavior and on its ability to affect the modulation of proinflammatory mediators in ECs.

Previous observations had shown that gremlin triggers VEGFR2-mediated intracellular signals that lead to in vitro EC sprouting and invasive activity and in vivo neovessel formation.<sup>30,32</sup> Here, we show that gremlin also exerts a proinflammatory response in ECs inducing NO production and an increase of intracellular cAMP levels that lead to EC permeability and CREB activation, respectively. Accordingly, a

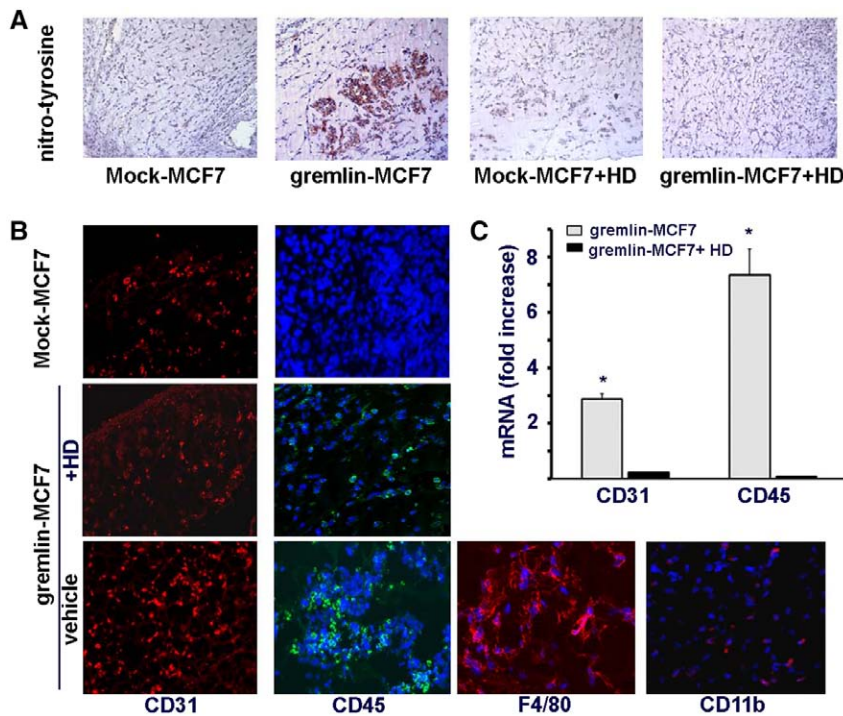


**Figure 7.** Hydrocortisone hampers the proinflammatory or proangiogenic activity exerted by gremlin-overexpressing tumor cells in mice. **A** and **B**, Mock- and gremlin-MCF7 cells were resuspended in Matrigel, implanted s.c. in 16-week-old nu/nu mice in the absence or in the presence of 10  $\mu$ g of hydrocortisone (HD) and examined at day 7. **A**, Anti-nitro-tyrosine immunostaining demonstrates that gremlin-MCF7 cells induce NO production in tumor grafts that is abolished hydrocortisone. **B**, Accordingly, note the presence of numerous CD31<sup>+</sup> endothelial cells and of CD45<sup>+</sup> infiltrating leukocytes, mainly consisting of F4/80<sup>+</sup> macrophages and fewer CD11b<sup>+</sup> monocytes, in gremlin-MCF7 grafts when compared with hydrocortisone-treated samples. Nuclei are shown by 4',6-diamidino-2-phenylindole counterstaining. Samples were analyzed using a Zeiss Axiovert 200M epifluorescence microscope equipped with Apotome system and an LD A PLAN 20X/0,30PH1 objective. **C**, Quantitative real time polymerase chain reaction analysis of the grafts confirms the inhibitory effect exerted by hydrocortisone on the proinflammatory or proangiogenic response elicited by gremlin-MCF7 cells. Data are the mean  $\pm$  SD of 6 plugs (\* $P$  < 0.05; Student *t* test).

preliminary transcriptome analysis of gremlin-treated ECs points to the capacity of this factor to induce a proinflammatory signature in endothelium by causing the upregulation of various inflammatory cytokines, chemokines, and leukocyte-adhesion molecules (Andres, article in preparation). All these molecules concur to leukocyte extravasation. Here, we have confirmed this observation by showing that gremlin stimulates monocyte transmigration by acting on ECs and inducing the coordinate upregulation of the monocyte/macrophage and neutrophil chemotactic chemokines Ccl2, Ccl7, and Cxcl1 and the expression of the cell adhesion molecules VCAM-1 and ICAM-1 on the EC surface. This is paralleled by increased EC permeability and acquisition of a motile phenotype.

All these effects were inhibited by transient transfection of ECs with a dominant-negative CREB mutant and by a CRE-decoy oligonucleotide. Indeed, gremlin causes CREB activation, nuclear translocation, and DNA binding in ECs through a productive gremlin-VEGFR2 interaction. PI-3K and PKC mediate CREB activation after VEGFR2 engagement by VEGF-A.<sup>12,17</sup> Our observations demonstrate a nonredundant role of VEGFR2-mediated mitogen activated protein kinase and Src signaling in CREB activation by gremlin, whereas no effect was exerted by the PI-3K inhibitors LY294002 and Wortmannin or the PKC inhibitor GF109203X (data not shown). Together with the different kinetics of CREB activation by the 2 factors, these data reveal the previously unrecognized capacity of gremlin to trigger VEGFR2-dependent intracellular events distinct from those elicited by VEGF-A. This is in keeping with the different nanomechanical affinity of the 2 ligands for VEGFR2 because of different surface intermolecular interactions that may lead to distinctive EC responses (see reference 31 for a further discussion of this point).

Vascular permeability can be regulated by growth factors such as VEGF as well as by a wide array of inflammatory

mediators via distinct molecular processes.<sup>46</sup> Here, we show that CREB activation by gremlin, either when administered as a recombinant protein or when produced by tumor cells, drives the breakdown of EC barrier function in vitro and in vivo, paralleled by the redistribution of the major endothelial adherens junction protein vascular endothelial-cadherin and the tight junction-associated protein ZO-1, thus allowing protein diffusion through the EC monolayer and leukocyte transendothelial migration. Also, in keeping with the critical role of NO in modulating vascular permeability,<sup>47</sup> the NO-synthase inhibitor L-NAME hampers EC junction disassembly after gremlin stimulation. Moreover, we cannot rule the possibility that additional factors produced by gremlin-stimulated ECs may concur with gremlin in inducing vascular leakage. Further experiments are required to fully elucidate the mechanisms leading to gremlin-mediated EC permeability.

The upregulation of ICAM-1 and VCAM-1 in cytokine-activated ECs may occur via CREB activation as well as via the activation of the transcription factor NF- $\kappa$ B.<sup>40,41</sup> Indeed, NF- $\kappa$ B triggers a proinflammatory/proangiogenic transcription program in endothelium and regulates the production of various angiogenic factors<sup>48</sup> pointing to a tight cross-talk between NF- $\kappa$ B and CREB activity during inflammation.<sup>49</sup> Previous observations had shown the ability of gremlin to induce NF- $\kappa$ B activation in ECs, leading to Ang-1 upregulation.<sup>50</sup> Here, we demonstrate the role of CREB in the modulation of ICAM-1 and VCAM-1 expression in gremlin-activated ECs and its involvement in monocyte/macrophage transendothelial migration. Of note, EC treatment with the cAMP analogous dibutyryl-cAMP fails to recapitulate the proinflammatory response elicited by gremlin (Figure X in the online-only Data Supplement). Together, the data raise the possibility that NF- $\kappa$ B may concur with CREB activation in driving the proinflammatory phenotype triggered by gremlin in ECs.



However, the capacity of gremlin to induce the activation of 2 major proinflammatory transcription factors in ECs underlines the role of inflammation in the neovascularization process. This is confirmed by the ability of the anti-inflammatory drug hydrocortisone to hamper the angiogenic activity exerted in vivo by gremlin or gremlin-overexpressing tumor cells.

Gremlin may exert a dual role in different physiological and pathological conditions by acting as a BMP antagonist and as a noncanonical VEGFR2 ligand. For example, gremlin seems to play BMP-independent angiogenic and tumorigenic functions in different neoplasms<sup>25,26</sup> and to promote tumor epithelial-to-mesenchymal transition by inhibiting BMP signaling.<sup>51</sup> Although its contribution to neovascularization and tumor growth in experimental and human neoplasms deserves further investigation, our data support the notion that gremlin produced by tumor cells may induce angiogenesis by interacting directly with ECs and by stimulating the recruitment of a proangiogenic inflammatory infiltrate. Accordingly, previous observations have shown that gremlin upregulation may play a pathogenic role in different chronic inflammatory conditions, including hypoxic pulmonary hypertension,<sup>52</sup> diabetic nephropathy,<sup>53</sup> and lung fibrosis.<sup>54</sup> Indeed, gremlin haplodeficiency reduces vascular remodeling in hypoxic lung and diabetes mellitus-associated kidney damage.<sup>55</sup> However, gremlin attenuates atherosclerotic plaque growth in ApoE<sup>-/-</sup> mice<sup>56</sup> and may act as neuroprotective factor for dopamine neuron degeneration.<sup>57</sup> Thus, the biological impact of gremlin downregulation or of its overexpression in different pathological settings seems to be strictly contextual.

In conclusion, our data point to a nonredundant role of CREB in mediating the EC response to gremlin and underline the tight cross-talk between angiogenesis and inflammation (Figure XI in the online-only Data Supplement). The capacity of gremlin to activate a proinflammatory or proangiogenic phenotype in endothelium may contribute to neovascularization and activation of innate immune responses in different pathological conditions, including fibrosis and cancer.

### Acknowledgments

The contributions of authors in this study are as follows. M. Corsini, C. Ravelli, E. Moroni, E. Grillo, M. Presta, and S. Mitola designed research; M. Corsini, C. Ravelli, E. Moroni, E. Grillo, I.H. Ali, and S. Mitola performed research; M. Corsini, C. Ravelli, E. Moroni, E. Grillo, D.P. Brazil, M. Presta, and S. Mitola analyzed data; and M. Presta and S. Mitola wrote the article. We thank Drs C. Urbinati for helpful technical assistance and D. Ginty (Johns Hopkins University) for ACREB plasmid.

### Sources of Funding

This work was supported in part by grants from Ministero dell'Istruzione, Università e Ricerca (MIUR, Centro IDET, FIRB project RBAP11H2R9 2011) and Associazione Italiana per la Ricerca sul Cancro (AIRC grant n° 10396) to M. Presta and from MFAG n°9141 to S. Mitola.

### Disclosures

None.

### References

- Jackson JR, Seed MP, Kircher CH, Willoughby DA, Winkler JD. The codependence of angiogenesis and chronic inflammation. *FASEB J*. 1997;11:457–465.
- Carmeliet P, Jain RK. Angiogenesis in cancer and other diseases. *Nature*. 2000;407:249–257.
- Schmid MC, Varner JA. Myeloid cell trafficking and tumor angiogenesis. *Cancer Lett*. 2007;250:1–8.
- Zijlstra A, Seandel M, Kupriyanova TA, Partridge JJ, Madsen MA, Hahn-Dantona EA, Quigley JP, Deryugina EI. Proangiogenic role of neutrophil-like inflammatory heterophils during neovascularization induced by growth factors and human tumor cells. *Blood*. 2006;107:317–327.
- Voronov E, Shouval DS, Krelm Y, Cagnano E, Benharroch D, Iwakura Y, Dinarello CA, Apte RN. IL-1 is required for tumor invasiveness and angiogenesis. *Proc Natl Acad Sci U S A*. 2003;100:2645–2650.
- Naldini A, Leali D, Pucci A, Morena E, Carraro F, Nico B, Ribatti D, Presta M. Cutting edge: IL-1 $\beta$  mediates the proangiogenic activity of osteopontin-activated human monocytes. *J Immunol*. 2006;177:4267–4270.
- Leali D, Dell'Era P, Stabile H, Sennino B, Chambers AF, Naldini A, Sozzani S, Nico B, Ribatti D, Presta M. Osteopontin (Eta-1) and fibroblast growth factor-2 cross-talk in angiogenesis. *J Immunol*. 2003;171:1085–1093.
- Aplin AC, Gelati M, Fogel E, Carnevale E, Nicosia RF. Angiopoietin-1 and vascular endothelial growth factor induce expression of inflammatory cytokines before angiogenesis. *Physiol Genomics*. 2006;27:20–28.
- Angelo LS, Kurzrock R. Vascular endothelial growth factor and its relationship to inflammatory mediators. *Clin Cancer Res*. 2007;13:2825–2830.
- Andrés G, Leali D, Mitola S, Coltrini D, Camozzi M, Corsini M, Belleri M, Hirsch E, Schwendener RA, Christofori G, Alcamí A, Presta M. A proinflammatory signature mediates FGF2-induced angiogenesis. *J Cell Mol Med*. 2009;13(8B):2083–2108.
- Ichiki T. Role of cAMP response element binding protein in cardiovascular remodeling: good, bad, or both? *Arterioscler Thromb Vasc Biol*. 2006;26:449–455.
- Mayo LD, Kessler KM, Pincheira R, Warren RS, Donner DB. Vascular endothelial cell growth factor activates CRE-binding protein by signaling through the KDR receptor tyrosine kinase. *J Biol Chem*. 2001;276:25184–25189.
- Jeon SH, Chae BC, Kim HA, Seo GY, Seo DW, Chun GT, Yie SW, Eom SH, Kim PH. The PKA/CREB pathway is closely involved in VEGF expression in mouse macrophages. *Mol Cells*. 2007;23:23–29.
- Morishita K, Johnson DE, Williams LT. A novel promoter for vascular endothelial growth factor receptor (flt-1) that confers endothelial-specific gene expression. *J Biol Chem*. 1995;270:27948–27953.
- Leonard MO, Howell K, Madden SF, Costello CM, Higgins DG, Taylor CT, McLoughlin P. Hypoxia selectively activates the CREB family of transcription factors in the *in vivo* lung. *Am J Respir Crit Care Med*. 2008;178:977–983.
- Abramovitch R, Tavor E, Jacob-Hirsch J, Zeira E, Amariglio N, Pappo O, Rechavi G, Galun E, Honigman A. A pivotal role of cyclic AMP-responsive element binding protein in tumor progression. *Cancer Res*. 2004;64:1338–1346.
- Zhao D, Desai S, Zeng H. VEGF stimulates PKD-mediated CREB-dependent orphan nuclear receptor Nurr1 expression: role in VEGF-induced angiogenesis. *Int J Cancer*. 2011;128:2602–2612.
- Kottakis F, Polytarchou C, Foltopoulou P, Sanidas I, Kampranis SC, Tschlis PN. FGF-2 regulates cell proliferation, migration, and angiogenesis through an NDY1/KDM2B-miR-101-EZH2 pathway. *Mol Cell*. 2011;43:285–298.
- Hoot KE, Oka M, Han G, Bottinger E, Zhang Q, Wang XJ. HGF upregulation contributes to angiogenesis in mice with keratinocyte-specific Smad2 deletion. *J Clin Invest*. 2010;120:3606–3616.
- Schroer K, Zhu Y, Saunders MA, Deng WG, Xu XM, Meyer-Kirchath J, Wu KK. Obligatory role of cyclic adenosine monophosphate response element in cyclooxygenase-2 promoter induction and feedback regulation by inflammatory mediators. *Circulation*. 2002;105:2760–2765.
- Scoditti E, Massaro M, Carluccio MA, Distanti A, Storelli C, De Caterina R. PPARgamma agonists inhibit angiogenesis by suppressing PKC $\alpha$  and CREB-mediated COX-2 expression in the human endothelium. *Cardiovasc Res*. 2010;86:302–310.
- Pearce JJ, Penny G, Rossant J. A mouse cerberus/Dan-related gene family. *Dev Biol*. 1999;209:98–110.
- Vitt UA, Hsu SY, Hsueh AJ. Evolution and classification of cystine knot-containing hormones and related extracellular signaling molecules. *Mol Endocrinol*. 2001;15:681–694.
- Murphy M, McMahon R, Lappin DW, Brady HR. Gremlins: is this what renal fibrogenesis has come to? *Exp Nephrol*. 2002;10:241–244.
- Namkoong H, Shin SM, Kim HK, Ha SA, Cho GW, Hur SY, Kim TE, Kim JW. The bone morphogenetic protein antagonist gremlin 1 is

- overexpressed in human cancers and interacts with YWHAH protein. *BMC Cancer*. 2006;6:74.
26. Sneddon JB, Zhen HH, Montgomery K, van de Rijn M, Tward AD, West R, Gladstone H, Chang HY, Morganroth GS, Oro AE, Brown PO. Bone morphogenetic protein antagonist gremlin 1 is widely expressed by cancer-associated stromal cells and can promote tumor cell proliferation. *Proc Natl Acad Sci U S A*. 2006;103:14842–14847.
27. Stabile H, Mitola S, Moroni E, Belleri M, Nicoli S, Coltrini D, Peri F, Pessi A, Orsatti L, Talamo F, Castronovo V, Waltregny D, Cotelli F, Ribatti D, Presta M. Bone morphogenic protein antagonist Dm/gremlin is a novel proangiogenic factor. *Blood*. 2007;109:1834–1840.
28. Baemans W, Van Hul W. Extracellular regulation of BMP signaling in vertebrates: a cocktail of modulators. *Dev Biol*. 2002;250:231–250.
29. Mitola S, Moroni E, Ravelli C, Andres G, Belleri M, Presta M. Angiopoietin-1 mediates the proangiogenic activity of the bone morphogenic protein antagonist Dm. *Blood*. 2008;112:1154–1157.
30. Mitola S, Ravelli C, Moroni E, Salvi V, Leali D, Ballmer-Hofer K, Zammataro L, Presta M. Gremlin is a novel agonist of the major proangiogenic receptor VEGFR2. *Blood*. 2010;116:3677–3680.
31. Maiolo D, Mitola S, Leali D, Oliviero G, Ravelli C, Bugatti A, Depero LE, Presta M, Bergese P. Role of nanomechanics in canonical and noncanonical pro-angiogenic ligand/VEGF receptor-2 activation. *J Am Chem Soc*. 2012;134:14573–14579.
32. Chiodelli P, Mitola S, Ravelli C, Oreste P, Rusnati M, Presta M. Heparan sulfate proteoglycans mediate the angiogenic activity of the vascular endothelial growth factor receptor-2 agonist gremlin. *Arterioscler Thromb Vasc Biol*. 2011;31:e116–e127.
33. Ravelli C, Mitola S, Corsini M, Presta M. Involvement of alphavbeta3 integrin in gremlin-induced angiogenesis. *Angiogenesis*. 2013;16:235–243.
34. Shaywitz AJ, Greenberg ME. CREB: a stimulus-induced transcription factor activated by a diverse array of extracellular signals. *Annu Rev Biochem*. 1999;68:821–861.
35. Cui H, Okamoto Y, Yoshioka K, et al. Sphingosine-1-phosphate receptor 2 protects against anaphylactic shock through suppression of endothelial nitric oxide synthase in mice. *J Allergy Clin Immunol*. 2013.
36. Sun Z, Li X, Massena S, et al. VEGFR2 induces c-Src signaling and vascular permeability *in vivo* via the adaptor protein TSAd. *J Exp Med*. 2012;209:1363–1377.
37. Ono H, Ichiki T, Ohtsubo H, Fukuyama K, Imayama I, Iino N, Masuda S, Hashiguchi Y, Takeshita A, Sunagawa K. CAMP-response element-binding protein mediates tumor necrosis factor- $\alpha$ -induced vascular cell adhesion molecule-1 expression in endothelial cells. *Hypertens Res*. 2006;29:39–47.
38. Yang L, Kowalski JR, Yacono P, Bajmoczy M, Shaw SK, Froio RM, Golan DE, Thomas SM, Luscinskas FW. Endothelial cell cortactin coordinates intercellular adhesion molecule-1 clustering and actin cytoskeleton remodeling during polymorphonuclear leukocyte adhesion and transmigration. *J Immunol*. 2006;177:6440–6449.
39. Wittchen ES. Endothelial signaling in paracellular and transcellular leukocyte transmigration. *Front Biosci (Landmark Ed)*. 2009;14:2522–2545.
40. Hadad N, Tuval L, Elgazar-Carmom V, Levy R. Endothelial ICAM-1 protein induction is regulated by cytosolic phospholipase A2 $\alpha$  via both NF- $\kappa$ B and CREB transcription factors. *J Immunol*. 2011;186:1816–1827.
41. Parry CM, Simas JP, Smith VP, Stewart CA, Minson AC, Efsthathiou S, Alcami A. A broad spectrum secreted chemokine binding protein encoded by a herpesvirus. *J Exp Med*. 2000;191:573–578.
42. Li BX, Yamanaka K, Xiao X. Structure-activity relationship studies of naphthol AS-E and its derivatives as anticancer agents by inhibiting CREB-mediated gene transcription. *Bioorg Med Chem*. 2012;20:6811–6820.
43. Coltrini D, Di Salle E, Ronca R, Belleri M, Testini C, Presta M. Matrigel plug assay: evaluation of the angiogenic response by reverse transcription-quantitative PCR. *Angiogenesis*. 2013;16:469–477.
44. Kiefer F, Siekmann AF. The role of chemokines and their receptors in angiogenesis. *Cell Mol Life Sci*. 2011;68:2811–2830.
45. Presta M, Dell’Era P, Mitola S, Moroni E, Ronca R, Rusnati M. Fibroblast growth factor/fibroblast growth factor receptor system in angiogenesis. *Cytokine Growth Factor Rev*. 2005;16:159–178.
46. Claesson-Welsh L, Welsh M. VEGFA and tumour angiogenesis. *J Intern Med*. 2013;273:114–127.
47. Durán WN, Breslin JW, Sánchez FA. The NO cascade, eNOS location, and microvascular permeability. *Cardiovasc Res*. 2010;87:254–261.
48. De Martin R, Hoeth M, Hofer-Warbinek R, Schmid JA. The transcription factor NF- $\kappa$ B and the regulation of vascular cell function. *Arterioscler Thromb Vasc Biol*. 2000;20:E83–E88.
49. Wen AY, Sakamoto KM, Miller LS. The role of the transcription factor CREB in immune function. *J Immunol*. 2010;185:6413–6419.
50. Mitola S, Moroni E, Ravelli C, Andres G, Belleri M, Presta M. Angiopoietin-1 mediates the proangiogenic activity of the bone morphogenic protein antagonist Dm. *Blood*. 2008;112:1154–1157.
51. Li Y, Wang Z, Wang S, Zhao J, Zhang J, Huang Y. Gremlin-mediated decrease in bone morphogenetic protein signaling promotes aristolochic acid-induced epithelial-to-mesenchymal transition (EMT) in HK-2 cells. *Toxicology*. 2012;297:68–75.
52. Costello CM, Cahill E, Rowan SC, Harkin S, Howell K, Leonard MO, Southwood M, Cummins EP, Fitzpatrick SF, Taylor CT, Morrell NW, Martin F, McLoughlin P. Gremlin plays a key role in the pathogenesis of pulmonary hypertension. *Circulation*. 2012;125:920–930.
53. Li G, Li Y, Liu S, et al. Gremlin aggravates hyperglycemia-induced podocyte injury by a TGF $\beta$ /smad dependent signaling pathway. *J Cell Biochem*. 2013;114:2101–2113.
54. Costello CM, Cahill E, Martin F, Gaine S, McLoughlin P. Role of gremlin in the lung: development and disease. *Am J Respir Cell Mol Biol*. 2010;42:517–523.
55. Roxburgh SA, Kattla JJ, Curran SP, O’Meara YM, Pollock CA, Goldschmeding R, Godson C, Martin F, Brazil DP. Allelic depletion of grem1 attenuates diabetic kidney disease. *Diabetes*. 2009;58:1641–1650.
56. Müller I, Schönberger T, Schneider M, et al. Gremlin-1 Is an Inhibitor of Macrophage Migration Inhibitory Factor and Attenuates Atherosclerotic Plaque Growth in ApoE-/- Mice. *J Biol Chem*. 2013;288:31635–31645.
57. Phani S, Jablonski M, Pelta-Heller J, Cai J, Iacovitti L. Gremlin is a novel VTA derived neuroprotective factor for dopamine neurons. *Brain Res*. 2013;1500:88–98.

## Significance

Angiogenesis and inflammation are processes that are closely related in several pathological conditions, including cancer. Gremlin, a pro-angiogenic molecule released by tumor cells, induces proinflammatory responses in endothelial cells via cAMP-response element-binding protein activation. Here, we show that cAMP-response element-binding protein mediates the early phases of gremlin-induced angiogenesis, including stimulation of endothelial cell motility and permeability, leading to leukocyte adhesion to endothelial cells and extravasation. The capacity of gremlin to activate a proinflammatory or proangiogenic phenotype in endothelium may contribute to neovascularization and activation of innate immune responses in different pathological conditions, including fibrosis and cancer.

# Arteriosclerosis, Thrombosis, and Vascular Biology



JOURNAL OF THE AMERICAN HEART ASSOCIATION

## **Cyclic Adenosine Monophosphate-Response Element-Binding Protein Mediates the Proangiogenic or Proinflammatory Activity of Gremlin**

Michela Corsini, Emanuela Moroni, Cosetta Ravelli, Germán Andrés, Elisabetta Grillo, Imran H. Ali, Derek P. Brazil, Marco Presta and Stefania Mitola

*Arterioscler Thromb Vasc Biol.* 2014;34:136-145; originally published online November 14, 2013;

doi: 10.1161/ATVBAHA.113.302517

*Arteriosclerosis, Thrombosis, and Vascular Biology* is published by the American Heart Association, 7272 Greenville Avenue, Dallas, TX 75231

Copyright © 2013 American Heart Association, Inc. All rights reserved.

Print ISSN: 1079-5642. Online ISSN: 1524-4636

The online version of this article, along with updated information and services, is located on the World Wide Web at:

<http://atvb.ahajournals.org/content/34/1/136>

Data Supplement (unedited) at:

<http://atvb.ahajournals.org/content/suppl/2013/11/14/ATVBAHA.113.302517.DC1>

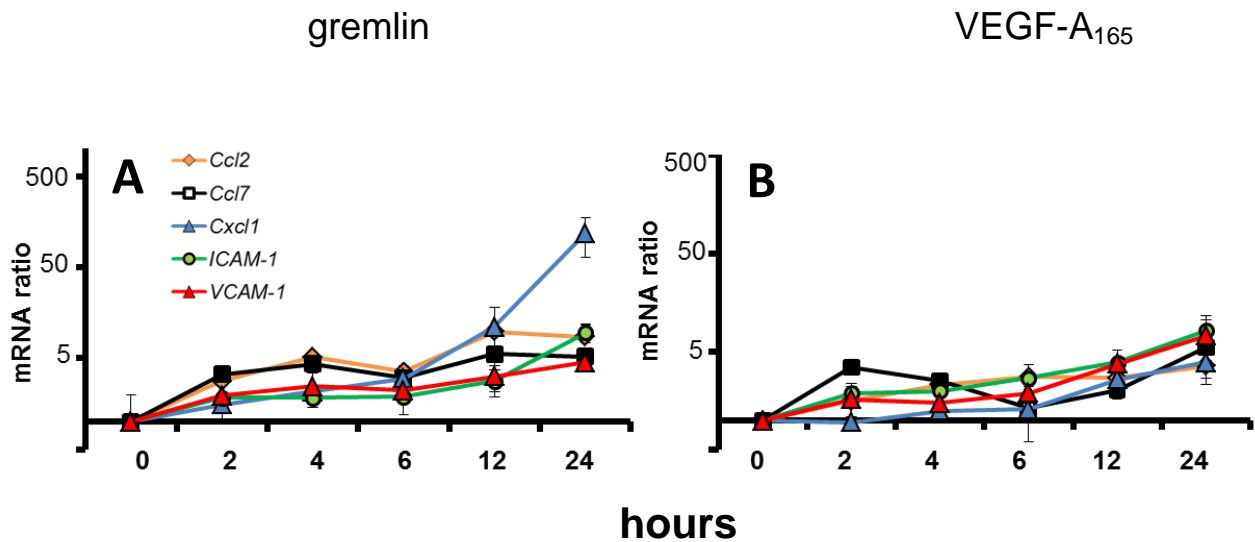
**Permissions:** Requests for permissions to reproduce figures, tables, or portions of articles originally published in *Arteriosclerosis, Thrombosis, and Vascular Biology* can be obtained via RightsLink, a service of the Copyright Clearance Center, not the Editorial Office. Once the online version of the published article for which permission is being requested is located, click Request Permissions in the middle column of the Web page under Services. Further information about this process is available in the [Permissions and Rights Question and Answer](#) document.

**Reprints:** Information about reprints can be found online at:  
<http://www.lww.com/reprints>

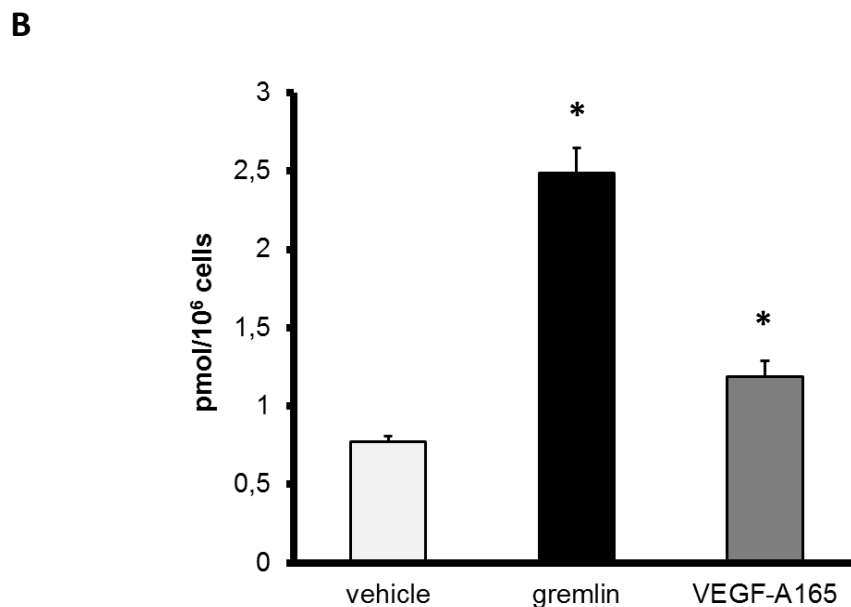
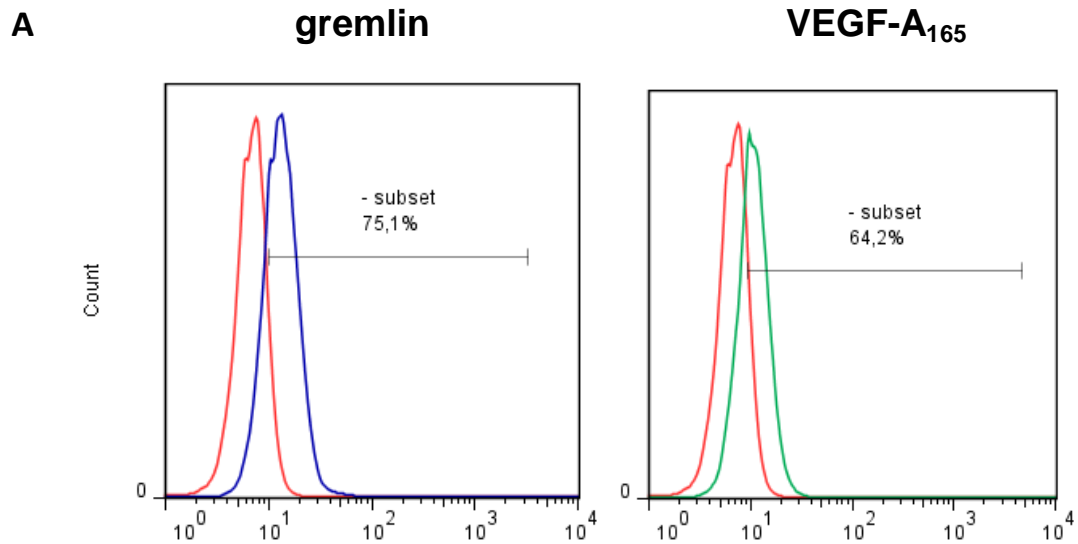
**Subscriptions:** Information about subscribing to *Arteriosclerosis, Thrombosis, and Vascular Biology* is online at:  
<http://atvb.ahajournals.org/subscriptions/>



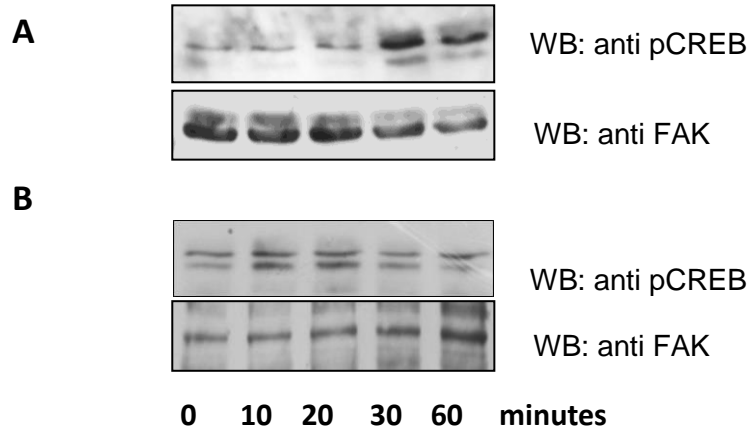
## SUPPLEMENTARY FIGURES



**Supplementary Figure I. Gremlin and VEGF-A<sub>165</sub> modulate the expression of chemokines and cell adhesion molecules in ECs.** Serum-starved SIECs were stimulated with 50 ng/mL of recombinant gremlin (A) or VEGF-A<sub>165</sub> (B) for 0, 2, 4, 6, 12 and 24 hours. At each time point total RNA was reverse transcribed to cDNA and analyzed by qRT-PCR. Data (mean values  $\pm$  SD; n= 3) represent the expression ratio of each target gene relative to the untreated control. Expression levels were normalized to  $\beta$ -actin expression.

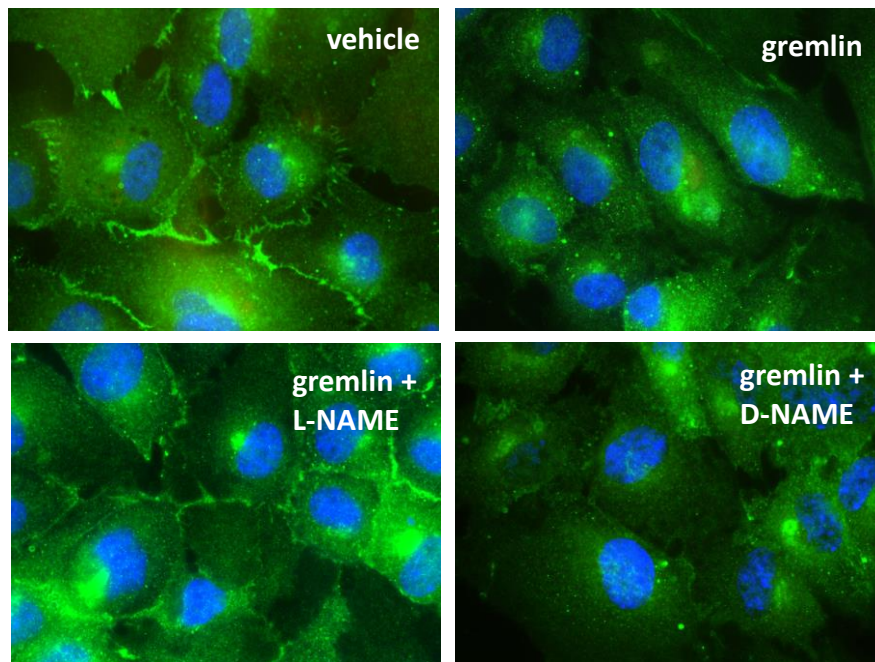


**Supplementary Figure II. Gremlin and VEGF-A<sub>165</sub> induce a pro-inflammatory response in ECs.** **A)** Fluorimetric determination of ROS production was carried out on SIECs ( $1 \times 10^6$  cells/sample) loaded with 5  $\mu$ M DCFH-DA and stimulated for 10 minutes with 50 ng/mL of gremlin (left panel) or VEGF-A<sub>165</sub> (right panel). Control cells (red line), 9.56% positive cells with  $6.61 \pm 2.1$  Geom. Mean; gremlin-stimulated cells (blue line), 75.1% positive cells with  $13.2 \pm 1.9$  Geom. Mean; VEGF-A<sub>165</sub>-stimulated cells (green line), 64.2% positive cells with  $10.4 \pm 2.3$  Geom. Mean (the values are the intensity mean of two independent experiments). **B)** non-acetylated cAMP levels were detected in SIEC lysates by competitive ELISA. To this purpose, SIECs were stimulated with 50 ng/mL of gremlin or VEGF-A<sub>165</sub> for 30 minutes and lysed in 0.1 M HCl. Data are the mean  $\pm$  SD from two independent experiments.

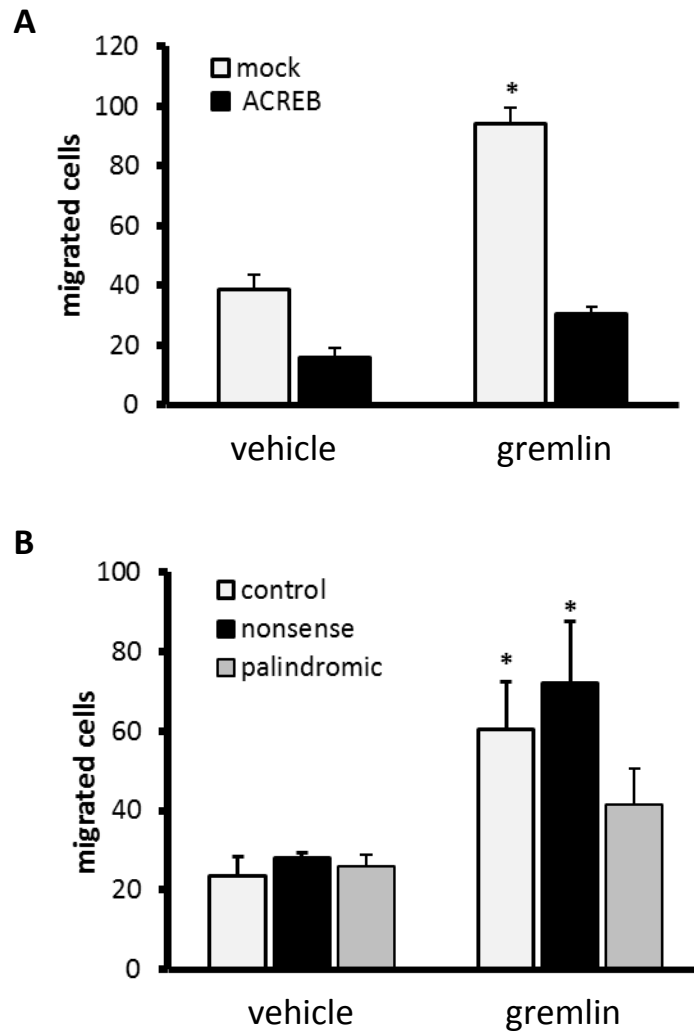


**Supplementary Figure III. Gremlin induces CREB activation in VEGFR2-expressing smooth muscle cells.** Calf aortic smooth muscle cells (**A**) and freshly isolated VEGFR1-expressing human PBMCs (**B**) were stimulated for 0 to 60 minutes with 50 ng/mL of recombinant gremlin. Then, 20  $\mu$ g aliquots of the cell lysates were probed by Western blotting with an anti-pCREB antibody. Uniform loading of the gels was confirmed by incubation of the membranes with anti-FAK antibodies.

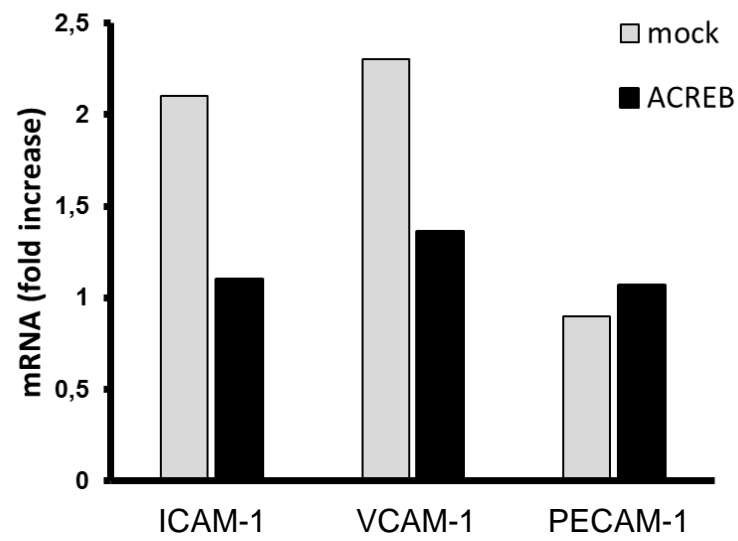




**Supplementary Figure IV. NO synthase inhibitor prevents EC junction disruption in gremlin-stimulated cells.** Confluent HUVECs were incubated with vehicle or 50 ng/mL of gremlin in the absence or in the presence of 100  $\mu$ M of the NO synthase inhibitor L-NAME or control D-NAME (Sigma), fixed with 3% PAF and permeabilized with 0.2% Triton X-100. Then, cells were incubated with anti-VE-Cad antibodies followed by anti-mouse Alexa 488. Nuclei were counterstained with DAPI. Note the capacity of L-NAME to prevent the disorganization of VE-Cad-positive EC junctions induced by gremlin. No effect was instead exerted by control D-NAME. Analysis was performed using a Zeiss Axiovert 200M epifluorescence microscope equipped with Apotome system and a Plan-Apochromat 63x/1.4 NA oil objective.

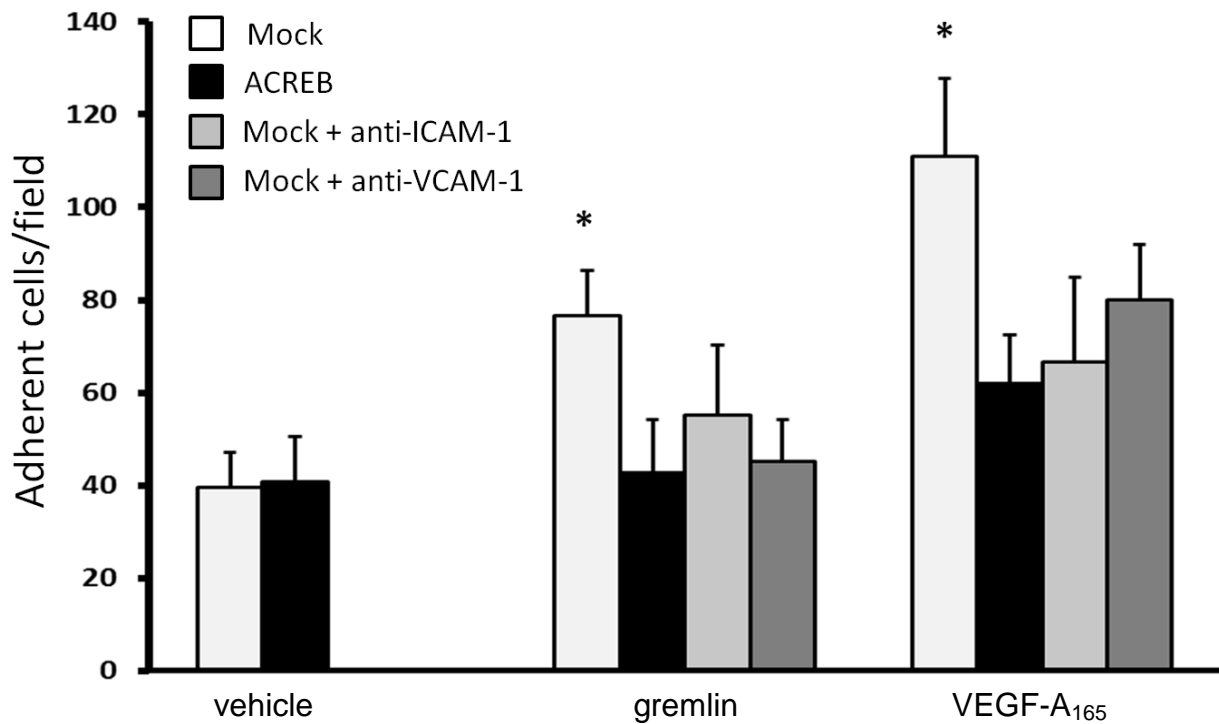


**Supplementary Figure V. CREB modulates gremlin-induced EC motility. A)** Mock and ACREB-SIECs were assessed for their capacity to migrate in response to 50 ng/mL of gremlin in a Boyden chamber assay. After 4 hours, cells migrated to the lower side of the filter were counted (\*,  $P < 0.05$  stimulated versus untreated; Student's  $t$  test). **B)** HUVECs were transfected with a CRE-decoy palindromic oligonucleotide or with control or nonsense oligonucleotides and tested in the Boyden chamber assay for their capacity to migrate through a gelatin-coated filter in response to 50 ng/mL gremlin. After 5 hours, cells migrated to the lower side of the filter were counted. (\*,  $P < 0.05$  stimulated versus untreated; Student's  $t$  test).

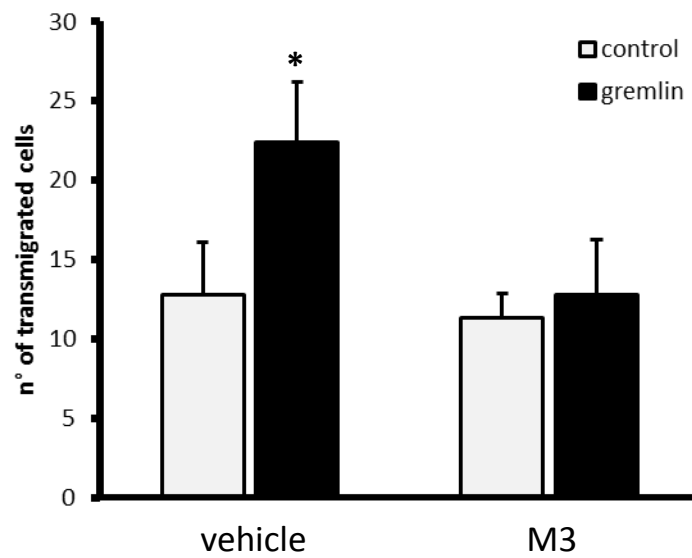


**Supplementary Figure VI)** Mock- and ACREB-transfected HUVECs were treated for 24 hours with 50 ng/mL of VEGF-A<sub>165</sub>. Then, ICAM-1, VCAM-1 and PECAM-1 mRNA levels were assessed by quantitative RT-PCR analysis.



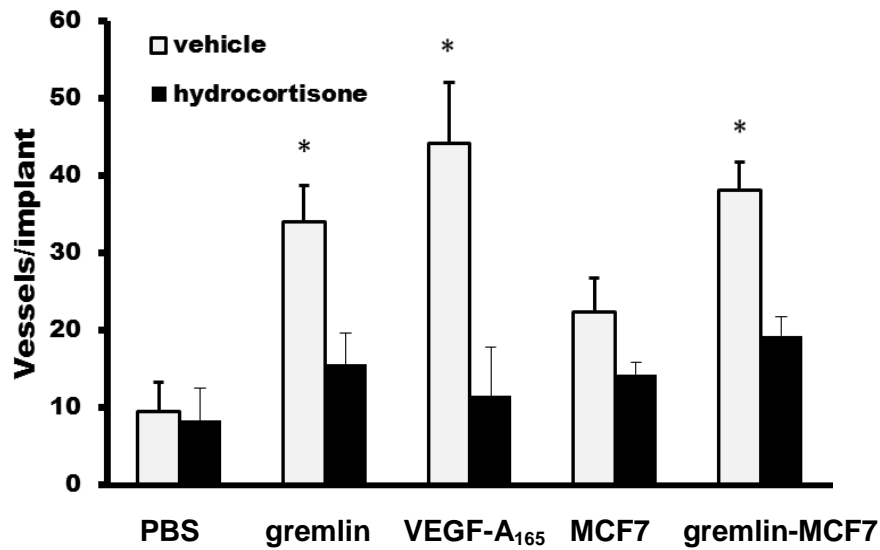


**Supplementary Figure VII. CREB mediates leukocyte adhesion induced by recombinant gremlin and VEGF-A<sub>165</sub>.** Mock- and ACREB-transfected HUVECs were treated for 24 hours with 50 ng/mL of recombinant gremlin or VEGF-A<sub>165</sub>. In parallel, mock cells were treated with gremlin or VEGF-A<sub>165</sub> in the presence of neutralizing anti-ICAM-1 or anti-VCAM-1 antibodies 10ug/mL. Then cells were incubated with LPS-activated THP-1 cells for 1 hour. At the end of the incubation, THP-1 cells adherent to the endothelium were counted in 5 random fields using Zeiss Axiovert 200M epifluorescence microscope equipped with LD A PLAN 20X/0.30PH1 objective. Data are the mean  $\pm$  S.D. of 3 determinations (\*,  $P < 0.05$ ; Student's t test).

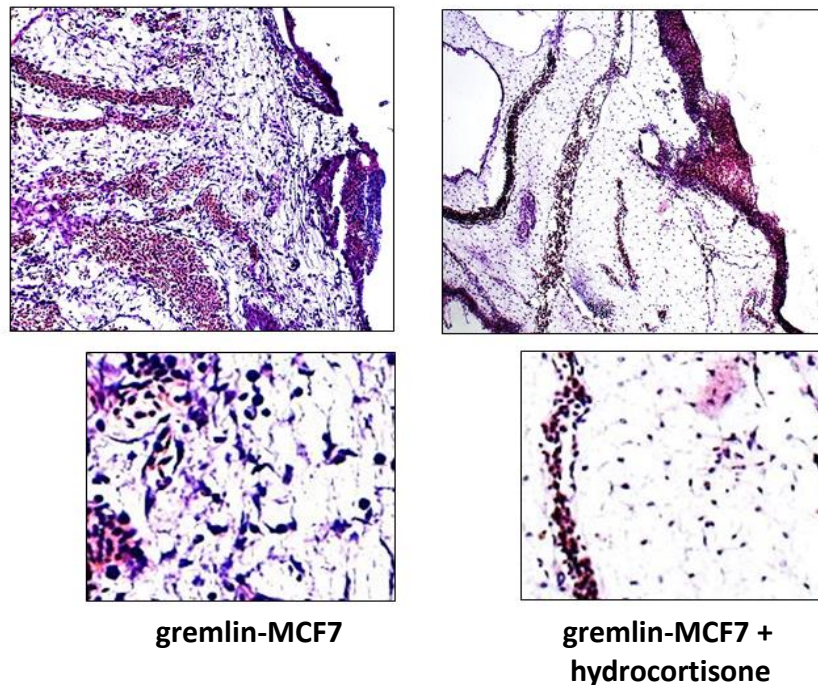


**Supplementary Figure VIII. The pan-chemokine inhibitor M3 hampers trans-endothelial migration of monocytic THP-1 cells induced by gremlin.** HUVECs were plated on a Transwell® membrane support and co-cultured for 24 hours with mock-MCF7 or gremlin-MCF7 cells seeded in the lower chamber. LPS-activated monocytic THP-1 cells were added to the upper chamber in the absence or in the presence of M3 (1.0 nM). Transmigrated monocytes were counted in 5 random fields. Data are the mean  $\pm$  S.D. of 3 determinations. (\*,  $P < 0.05$  stimulated versus untreated; Student's t test).

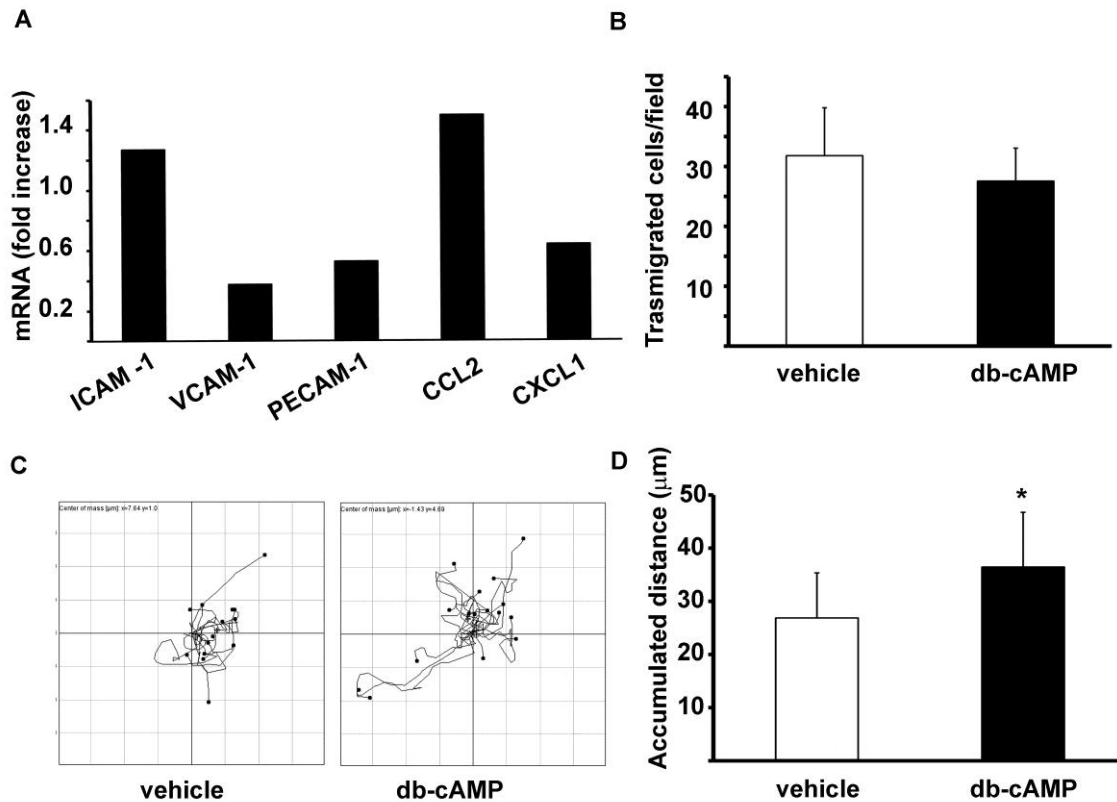
**A**



**B**

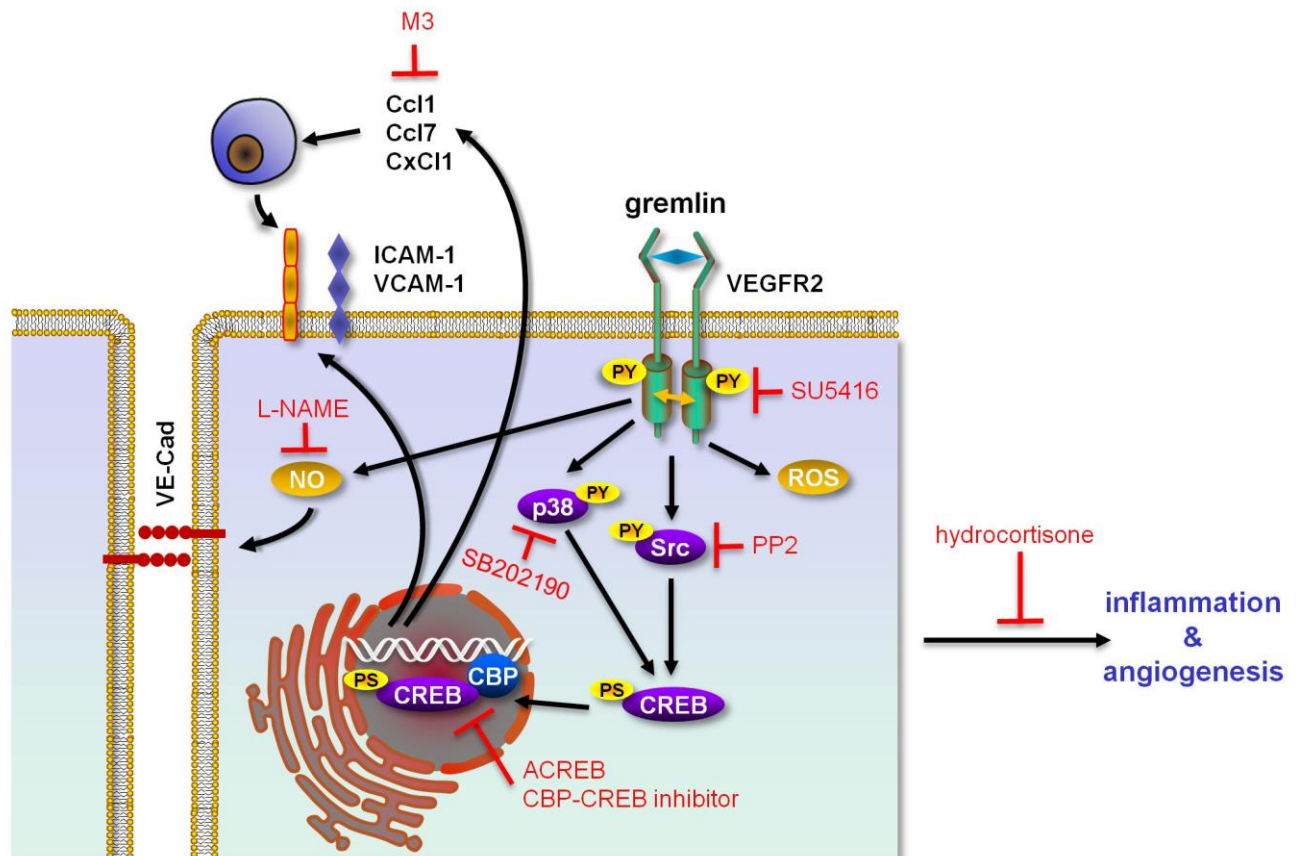


**Supplementary Figure IX. Hydrocortisone inhibits the pro-angiogenic response of gremlin and VEGF-A<sub>165</sub> in the chick embryo CAM.** **A)** Alginate pellets containing 100 ng of gremlin or VEGF-A<sub>165</sub> or 3  $\mu$ l of fivefold concentrated conditioned medium from mock and gremlin-MCF7 cells were implanted on the top of chick embryo CAMs at day 11 of development in the absence or in the presence of 1.0  $\mu$ g of hydrocortisone. After 3 days, newly formed microvessels converging towards the implant were counted at 5x magnification using a STEMI SR stereomicroscope equipped with an objective f equal to 100 mm with adapter ring 475070 (Carl Zeiss). **B)** Hematoxylin/eosin staining of paraffin-embedded chick embryo CAMs at day 11 of development treated with the conditioned medium from mock and gremlin-MCF7 in the absence or in the presence of 1.0  $\mu$ g of hydrocortisone. Samples were analyzed using a Zeiss Axiovert 200M epifluorescence microscope equipped with Apotome system and an ACROPLAN 10X/0,25 (top panel) and with a LD A PLAN 20X/0,30PH1 objectives (bottom panel). Note the presence of an abundant inflammatory cell infiltrate in the areas of gremlin-induced neovascularization abolished by hydrocortisone treatment, as evidenced in lower panels at enlarged magnification



**Supplementary Figure X. db-cAMP administration does not recapitulate the pro-inflammatory effects of gremlin on ECs.** **A)** HUVECs were treated for 24 hours with 2  $\mu$ M of db-cAMP. Then, ICAM-1, VCAM-1 and PECAM-1 mRNA levels were assessed by quantitative RT-PCR analysis. **B)** HUVECs were plated on a Transwell® membrane support in the absence or in the presence of 2  $\mu$ M db-cAMP. LPS-activated THP-1 cells were added to the upper chamber and transmigrated THP-1 cells were counted in 5 random fields using a Zeiss Axiovert 200M epifluorescence microscope equipped with LD A PLAN 20X/0,30PH1 objective. Data are the mean  $\pm$  S.D. of 3 wells. **C-D)** HUVECs were seeded in M199 plus 5% FCS. Then, cells were stimulated with 2  $\mu$ M db-cAMP and cell motility was assessed by time lapse videomicroscopy using an inverted photomicroscope (Zeiss Axiovert 200M) equipped with a LD A PLAN 20X/0,30PH1 objective. Constant temperature (37°C) and pCO<sub>2</sub> (5%) were maintained throughout the experimental period by means of heatable stage and climate chamber. Phase-contrast snap photographs were digitally recorded for 240 minutes. Cell paths (15-20 cells per experimental point) were generated from centroid positions and migration parameters were analysed with the “Chemotaxis and Migration Tool” of ImageJ Software (<http://rsbweb.nih.gov/ij>). Representative tracked paths of HUVECs stimulated by vehicle or 2  $\mu$ M db-cAMP are shown in panel **C** and accumulated distances (in  $\mu$ m) are shown in panel **D**. (\*,  $P < 0.05$ ; Student’s t test). Together, these data indicate that CREB activation by db-cAMP is not *per se* sufficient to recapitulate the pro-inflammatory effect of gremlin on ECs.





**Supplementary Figure XI. Schematic representation of the CREB-mediated pro-inflammatory/pro-angiogenic activity of gremlin.** By interacting with VEGFR2, gremlin activates different signal transduction pathways, leading to ROS and NO production and CREB phosphorylation. CREB activation causes the upregulation of different chemokines and cell-adhesion molecules, leading to leukocyte recruitment. In parallel, NO production affects EC junctions, increasing blood vessel permeability. The pro-inflammatory response plays a non-redundant role in mediating the angiogenic activity of gremlin, as shown by the inhibitory effect exerted by different approaches hampering VEGFR2 signaling, NO production, CREB activity, chemokine function and inflammation (in red).

## METHODS AND MATERIALS

### Cell cultures and transfection

Subcutaneous mouse microvascular ECs (SIECs, provided by A. Vecchi, Institute Humanitas, Milan, Italy) were cultured in Dulbecco's modified Eagle's medium (DMEM, Gibco Life Technologies, Grand Island, NY) supplemented with 10% heat-inactivated donor calf serum. Human umbilical vein ECs (HUVECs), prepared and characterized as described<sup>1</sup>, were grown in M199 medium (Gibco) supplemented with 20% fetal calf serum (FCS, Gibco), 100 µg/mL endothelial cell growth factor (Sigma Chemical Co. St. Louis, MO) and 100 µg/mL porcine heparin (Sigma). HUVECs were used at the second passage and grown on plastic surface coated with porcine gelatin (Sigma). When indicated, ECs were transiently transfected with the pcDNA3 expression vector harboring the mutant ACREB cDNA<sup>2</sup> (provided by D. Ginty, Johns Hopkins University, Baltimore, MD) or with the empty vector. Human monocytic THP-1 cells [American Type Culture Collection (ATCC), Manassas, VA] were cultured in RPMI 1640 medium supplemented with 10% heat-inactivated FCS, 100 U/mL penicillin, 100 µg/mL streptomycin, and 2.0 mM L-glutamine. Human adenocarcinoma breast cancer MCF7 cells (HTB-22, ATCC) were grown in DMEM containing 10% FCS, vitamins, essential and non-essential amino acids. MCF7 cells were transfected with the pcDNA3 vector harbouring the human gremlin cDNA or with the empty vector by standard procedures to generate stable gremlin-MCF7 and mock-MCF7 cell populations, respectively. Cell cultures were maintained at 37°C in a humidified atmosphere containing 5% CO<sub>2</sub>.

### Quantitative RT-PCR

Three independent SIEC cultures were stimulated for different time points ranging between 2 hours and 24 hours with 50 ng/mL of murine gremlin (R&D System, Minneapolis, MN) or with 50 ng/mL of human VEGF-A<sub>165</sub> (provided by K. Ballmer-Hofer, Paul Scherrer Institut, Switzerland) in DMEM supplemented with 2% serum. Steady-state transcription levels of selected genes were evaluated in SIECs by quantitative real-time RT-PCR (qRT-PCR). In brief, total RNA was isolated using TRIzol Reagent (Invitrogen, Carlsbad, CA) according to manufacturer's instructions. Four µl of total RNA were retro-transcribed with M-MLV reverse transcriptase (Invitrogen) using random hexaprimers in a final 20 µl volume. Quantitative PCR was performed with a Biorad iCycler iQ™ Real-Time PCR Detection System using a iQ™ SYBR Green Supermix (Biorad, Hercules, CA) according to manufacturer's instructions. Each PCR reaction was performed in triplicate on one plate and fluorescence data were recorded using iCycler software (BioRad). Relative expression ratios were calculated by use of Pfaffl equation and Relative Expression Software Tool. The mRNA expression levels of target genes were normalized to the levels of β-actin transcript.

The following specific primers were used:

Ccl2 (NM_011333):	5'-CTTCTGGGCCTGCTGTTCA-3' (forward), 5'-CCAGCCTACTCATTGGGATCA-3' (reverse);
Ccl7 (NM_013654):	5'-CCTGGGAAGCTGTTATCTTCA-3' (forward), 5'-TTGGCTCCTAGGTTGGTTTC-3' (reverse);
Cxcl1 (NM_008176):	5'-ACCGAAGTCATAGCCACACTC-3' (forward), 5'-CTCCGTTACTTGGGGACACC-3' (reverse);
VCAM-1 (NM_011693):	5'-GAACTGATTATCCAAGTCTCTCCA-3' (forward), 5'-GAACTGATTATCCAAGTCTCTCCA-3' (reverse);
ICAM-1 (NM_010493):	5'-CACGTGCTGTATGGTCCTCG-3' (forward), 5'-TAGGAGATGGGTTCCCCCAG-3' (reverse);
β-actin (NM_009073):	5'-CGTAAAGACCTCTATGCCAACA-3' (forward), 5'-CCACCGATCCACACAGAGTA-3' (reverse).

### **Intracellular signaling**

Confluent SIECs were made quiescent by a 20 hours-starvation in serum-free or 5% FCS-supplemented medium. After stimulation with 50 ng/mL of gremlin or VEGF-A<sub>165</sub>, cells were lysed and 20 µg aliquots were analyzed by 6% or 10% SDS-PAGE followed by Western blotting with antibodies against pCREB (pSer-133, Cell Signaling Technology, Beverly, MA), CREB, pERK1/2 or FAK (Santa Cruz Biotechnology, Santa Cruz, CA).

### **EMSA and *in situ* CREB/DNA binding assay**

Nuclear extracts from control and gremlin-stimulated HUVECs were prepared using the Nuclear and Cytoplasmic Extraction Kit (Active Motif, Rixensart, Belgium). Then, 2 µg aliquots of nuclear extracts were incubated for 20 minutes at room temperature with a biotin-labeled, double-stranded, gene-specific wild-type probe (sense, 5'-AGAGATTGCCTGACGTCAGAGAGTAG-3') in the absence or in the presence of a molar excess of the unlabeled-probe or of a mutated one (sense, 5'-AGAGATTGCCTGTGGTCAGAGAGTAG-3') or of anti-CREB antibodies according to the LightShift Chemiluminescent EMSA Kit instructions (Pierce, Rockford, IL USA). Samples were then loaded onto 6 % non-denaturing polyacrylamide gel and electrophoresed in Tris-borate-EDTA buffer. The DNA-binding activity of CREB was also assessed in HUVECs by ELISA (TransAM™; Transcription Factor ELISA kit pCREB (#43096; Active Motif, Carlsbad, CA) using nuclear protein extracts according to the Transcription Factor ELISA kit instructions.

For *in situ* CREB/DNA binding assay, samples were fixed in 3% paraformaldehyde/2% sucrose in PBS, permeabilized with 0.5% Triton-X100 and incubated with Cy5-labeled probe (5'-AGAGATTGCCTGACGTCAGAGAGTAG-3') or Cy5-labeled mutated probe (5'-AGAGATTGCCTGTGGTCAGAGAGTAG-3') and analyzed using a Zeiss Axiovert 200M epifluorescence microscope equipped with a Plan-Apochromat 63x/1.4 NA oil objective.

### **EC immunofluorescence analysis**

HUVECs were seeded on gelatin-coated glass coverslips in DMEM added with 2% FCS. After overnight incubation, cells were treated with gremlin or VEGF-A<sub>165</sub> for 0-30 minutes at 37°C, washed, fixed in 3% paraformaldehyde/2% sucrose in PBS, permeabilized with 0.5% Triton-X100, and saturated with goat serum in PBS. Then, cells were incubated with anti-pCREB antibody (pSer-133, Cell Signaling Technology), or with anti-ZO-1 (Invitrogen) or anti-Ve-Cadherin (Santa Cruz) antibody followed by Alexa Fluor 488 anti-rabbit IgG (Molecular Probes, Eugene, OR). Nuclei were counterstained with 4',6-diamidino,2-phenylindole (DAPI, Sigma). Cells were analyzed using a Zeiss Axiovert 200M epifluorescence microscope equipped with Apotome and a Plan-Apochromat 63x/1.4 NA oil objective.

### **EC motility assay**

HUVEC motility was assessed by time lapse videomicroscopy. To this purpose, mock and ACREB-transfected HUVECs were seeded in 24 well-plates at 150 cells/mm<sup>2</sup>. After 2 hours, cells were stimulated with gremlin or VEGF-A<sub>165</sub> dissolved in M199 (Gibco) plus 0.5% FCS. Constant temperature (37°C) and 5% CO<sub>2</sub> were maintained throughout the experimental period by means of an heatable stage and climate chamber. Cells were observed under an inverted photomicroscope (Zeiss Axiovert 200M) and phase-contrast snap photographs (one frame every 10 minutes) were digitally recorded for 240 minutes. Cell paths (25-30 cells per experimental point) were generated from centroid positions and migration parameters were analysed with the "Migration and Chemotaxis" tool of ImageJ Software (<http://rsbweb.nih.gov/ij>).

### **EC chemotaxis assay**

ECs were seeded at  $1.0 \times 10^6$  cells/mL in the upper compartment of a Boyden chamber containing gelatin-coated PVP-free polycarbonate filters (5  $\mu$ m pore size, Costar, Cambridge, MA). Gremlin dissolved in M199 with 1% FCS was placed in the lower compartment. 1% FCS medium was used as negative control. After 5 hours of incubation at 37°C, cells migrated to the lower side of the filter were stained with Diff-Quik (Dade-Behring, Milan, Italy). Five random fields were counted for each triplicate sample.

### **Fluorimetric analysis of intracellular ROS**

Intracellular ROS levels were determined by measuring fluorescence intensity (excitation at 475 nm, emission at 525 nm) in cells suspended in serum-free medium and loaded with the redox-sensitive dye DCFH-DA (Molecular Probe, Life Technology). The nonfluorescent DCFH-DA readily diffuses into the cells where it is hydrolyzed to the polar derivative DCFH, which is in turn oxidized in the presence of  $H_2O_2$  to the highly fluorescent DCF. Cells ( $1 \times 10^6$ ) were incubated with 5  $\mu$ M DCFH-DA in the dark at 37°C. After 30 minutes of incubation, cells were washed with a pulse spin and immediately suspended in 1 mL of PBS. FACS analysis was performed with a CyFlow Partec flow cytometer (Partec Italia, Milano, Italy) and data were analysed with FlowJo software (Ashland, OR).

### **cAMP competitive ELISA**

SIEC ( $6 \times 10^4$  cells/well in a 48 well plate) were washed with Hanks Balanced Salt Solution (Gibco), 20 mM HEPES (Gibco), in presence of 1 mM IBMX (3-isobutyl-1-methylxanthine, Sigma) and stimulated with gremlin or VEGF-A<sub>165</sub> for 30 minutes. Then, cells were lysed in 150  $\mu$ L of 0.1N HCl for 10 minutes at room temperature. cAMP was measured using a cAMP competitive ELISA (Thermo Scientific) according to manufacturer's instruction.

### **EC permeability assay**

Mock- and ACREB-transfected ECs were plated at confluence on gelatin-coated Transwell® membrane support (0.3  $\mu$ m pore size, 6.5-mm diameter, polyester filters; Millipore) at the density of  $2.5 \times 10^4$  cells/well. Then, endothelial monolayers were treated with the conditioned medium from mock-MCF7 or gremlin-MCF7 cells for 24 hours. To measure EC permeability, biotin-BSA was added to the top chamber at 50  $\mu$ g/well. After 90 min, the top chamber was removed, and biotin-BSA was measured in the lower chamber with horseradish peroxidase (HRP)-conjugated streptavidin (GeHealthcare Life Science, Milan, Italy).

### **Miles vascular permeability assay**

Evan's blue dye (Sigma) (100  $\mu$ L of 1% solution in 0.9% NaCl) was injected intravenously into 6-8 week-old C57BL6 mice (Charles River, Calco, Italy). After 10 minutes, 50  $\mu$ L of recombinant gremlin or VEGF-A<sub>165</sub> (both at 1 ng/ $\mu$ L concentration) were injected intradermally into the shaved back skin. After 20 minutes, the animals were sacrificed and an area of the skin that included the entire injection site was removed. Evan's blue dye was extracted from skin by incubation with formamide (Sigma) for 5 days at room temperature and measured at 620 nm.

### **Monocyte-EC adhesion assay**

Confluent monolayers of mock- and ACREB-HUVECs were treated with the conditioned medium from mock-MCF7 or gremlin-MCF7 cells or with 50 ng/mL of gremlin or VEGF-A<sub>165</sub> for 24 hours. Then, LPS-activated THP-1 monocytes were loaded with 8  $\mu$ M CellTracker Green (CMFDA; Invitrogen) for 1 hour at 37°C and added at  $1 \times 10^6$  cells/well on the top of the endothelial

monolayers. After 30 minutes of incubation at 37°C, non-adherent THP-1 cells were removed with a PBS wash and adherent cells were quantified in 5 random fields per sample under a Zeiss Axiovert 200M epifluorescence microscope.

### **Monocyte trans-endothelial migration assay**

Mock- and ACREB-HUVECs seeded on 6.5 mm polyester Transwell® inserts (3.0 µm pore size) were grown to confluence. Then, mock-MCF7 or gremlin-MCF7 cells were seeded in the lower chamber and co-cultured with HUVEC monolayers for 24 hours. At the end of the incubation, LPS-activated THP-1 monocytes were added at  $1 \times 10^6$  cells/well on the top of the endothelial monolayers. After 16 hour of incubation at 37°C, Transwell® inserts were removed and endothelial-transmigrated cells were quantified in 5 random fields per sample under a Zeiss Axiovert 200M epifluorescence microscope.

### **Chick embryo chorioallantoic membrane (CAM) assays**

In a first set of experiments, 100 µL of PBS with or without 100 ng of recombinant gremlin were pipetted on the top of the CAM of fertilized White Leghorn chicken eggs at day 11 of incubation. After 20 minutes, CAMs were stained for in situ CREB/DNA binding with the Cy5-labeled probe (5'-AGA GAT TGC CTG ACG TCA GAG AGC TAG-3') or Cy5-labeled mutated probe (5'-AGA GAT TGC CTG TGG TCA GAG AGC TAG-3') as described above and analyzed using a Zeiss Axiovert 200M epifluorescence microscope. In further experiments, 100 ng/pellet of gremlin or VEGF-A<sub>165</sub> were placed on top of day 11 CAMs at in the absence or in the presence of 5 µM CBP-CREB interaction inhibitor (Calbiochem). After 3 days, inflammatory cell infiltrate was assessed by H&E staining of paraffin-embedded CAM sections. Finally, conditioned medium from mock-MCF7 and gremlin-MCF7 cells were collected and concentrated fivefold using Centricon YM-10 filters (Millipore, Billerica MA). Alginate beads containing the concentrated conditioned medium (3 µL) or 100 ng/pellet of gremlin or VEGF-A<sub>165</sub> were placed on top of the CAMs in the absence or in the presence of 1 µg of hydrocortisone. After 3 days, newly formed microvessels converging towards the implant were counted at 5x magnification using a STEMI SR stereomicroscope equipped with an objective f equal to 100 mm with adapter ring 475070 (Carl Zeiss).

### **In vivo murine pro-inflammatory/pro-angiogenic activity assays**

The pro-inflammatory/pro-angiogenic activity of gremlin was assessed by the murine Matrigel plug assay. To this purpose, liquid growth factor reduced Matrigel (9 mg of protein/mL; Cultrex BME, Gaithersburg, MD) was mixed at 4°C with gremlin or VEGF-A<sub>165</sub> at a final concentration of 1.0 µg/mL in the absence or in the presence of 10 µg of hydrocortisone and injected subcutaneously (0.4 mL/mouse) into the flank of 6-8 week-old C57BL6 mice. One week after injection, plugs were harvested and the pro-inflammatory/pro-angiogenic response was quantified by qRT-PCR as described<sup>4</sup>. Briefly, total RNA was extracted from Matrigel plugs using TRIzol reagent according to manufacturer's instructions (Invitrogen, Carlsbad, CA). Before RNA extraction, plugs were added with an appropriate volume of TRIzol solution containing tracer human cells to a final concentration of  $1 \times 10^4$  cells per mg of Matrigel. Purified total RNA were dissolved in RNase free water (1 µL per mg of Matrigel). The mRNA expression levels of target genes were normalized to the levels of human GAPDH housekeeping gene. In each experiment, an arbitrary value equal to 1.0 was assigned to the levels of expression of the gene(s) measured in one PBS plug that was used as reference sample. In parallel experiments, plugs were analyzed immunohistochemically for the presence of inflammatory cells and newly formed blood vessels as described<sup>3</sup>.



### **In vivo tumor xenograft assay**

Athymic nu/nu nude male mice (Charles River, Calco, Italy) were injected s.c. with 400  $\mu$ L of growth factor reduced Matrigel containing  $3 \times 10^5$  gremlin-MCF7 or mock-MCF7 cells (4 animals per group, 2 plugs per animal) in the absence or in the presence of 10  $\mu$ g of hydrocortisone. After 7 days, Matrigel plugs were collected and divided in two parts. One-half was embedded in Tissue Tec OCT (Sigma), snap frozen by immersion in liquid nitrogen-cooled isopentane and analyzed by immunofluorescence microscopy as described <sup>3</sup>. The other half was processed for total RNA extraction and qRT-PCR analysis as described <sup>4</sup>.

### **REFERENCES**

1. Mitola S, Moroni E, Ravelli C, Andres G, Belleri M, Presta M. Angiopoietin-1 mediates the proangiogenic activity of the bone morphogenic protein antagonist Dm. *Blood*. 2008;112:1154-1157.
2. Ahn S, Olive M, Aggarwal S, Krylov D, Ginty DD, Vinson C. A dominant-negative inhibitor of CREB reveals that it is a general mediator of stimulus-dependent transcription of c-fos. *Mol Cell Biol*. 1998;18:967-977.
3. Andres G, Leali D, Mitola S, Coltrini D, Camozzi M, Corsini M, Belleri M, Hirsch E, Schwendener RA, Christofori G, Alcamì A, Presta M. A pro-inflammatory signature mediates FGF2-induced angiogenesis. *J Cell Mol Med*. 2009;13:2083-2108.
4. Coltrini D, Di Salle E, Ronca R, Belleri M, Testini C, Presta M. Matrigel plug assay: evaluation of the angiogenic response by reverse transcription-quantitative PCR. *Angiogenesis*. 2013;16:469-477.